FACTORS INFLUENCING PHOSPHORUS LOSSES IN AGROECOSYSTEMS DOMINATED BY TILE DRAINAGE

BY

LUIS F. ANDINO GALEANO

THESIS

Submitted in partial fulfillment of the requirements
for the degree of Master of Science in Natural Resources and Environmental Sciences
in the Graduate College of the
University of Illinois at Urbana-Champaign, 2019

Urbana, Illinois

Master's Committee:

Associate Professor Jennifer M. Fraterrigo, Adviser
Associate Professor Yuji Arai
Mr. Lowell Gentry

ABSTRACT

Phosphorus is an important macronutrient for crop production but phosphorus surpluses may be conveyed from diffuse sources to streams via surface runoff and artificial subsurface (perforated plastic pipes called tiles) drainage affecting the quality of receiving aquatic ecosystems. However, controls of phosphorus losses at the sub-field and watershed scales are not fully understood. The overall goal of this study is to determine the effect on phosphorus losses of topography, soil phosphorus, management practices, meteorological conditions, and hydrologic characteristics in agricultural fields and watersheds dominated by tile-drainage in central Illinois. First, tile dissolved reactive phosphorus yields and flow-weighted mean concentration were characterized from January 2015 through September 2017 to determine seasonal (growing vs non-growing) patterns from 36 individually monitored plots across a farm under a corn (*Zea mays* L.) and soybean (*Glycine max* L.) rotation. Tile dissolved reactive phosphorus yields increased with precipitation and were greatest during the non-growing season in 2016 and 2017. Annual tile dissolved reactive phosphorus yields were positively related to soil test phosphorus. During the non-growing season, there was a positive relationship between depression depth quantified at the plot-scale and tile dissolved reactive phosphorus yields and flow-weighted mean concentrations. Along depression gradients, piecewise regression displayed a threshold at a depression depth of 0.38 m at which soil test phosphorus increased, indicating soil phosphorus accumulation at the bottom of closed depressions. Then, I evaluated how hydrologic drivers (precipitation, water retention capacity, runoff, baseflow) affected phosphorus exports from three agricultural watersheds dominated by tile drainage using long-term datasets (range of 10 – 26 years of records). Water retention capacity expressed as the runoff: precipitation ratio was a better predictor of runoff as well as dissolved reactive phosphorus and particulate phosphorus

losses than precipitation. Power law relationships between particulate phosphorus loads and runoff indicated that particulate phosphorus losses increment exponentially during wet years. Additionally, I assessed the performance of the base and modified (including an antecedent flow anomaly term) weighted regressions on time, discharge, and season method to estimate phosphorus exports relative to observed data. The inclusion of the flow anomaly term to the base model did not improve the performance due to the influence of management practices and other physical properties of the watershed. Similarly, the base model needs improvement to estimate phosphorus losses.

ACKNOWLEDGEMENTS

My sincere gratitude to my adviser Jennifer Fraterrigo for her mentoring, guidance, dedication, understanding, patience, and for believing in me. Thanks to her academic, professional, and personal support I could complete this enriching experience. Thanks to my advisory committee, Lowell Gentry and Dr. Yuji Arai, for their academic and professional advice that shaped this project.

Thanks to Mark David, Lowell Gentry (one more time), and Corey Mitchell for giving me the opportunity to come (and stay) to the University of Illinois, for their mentoring, and unconditional support since 2011. Thanks to the talented and supportive Fraterrigo Lab (Matt Candeias, Sam Stickley, Mara Rembelski, Tyler Refsland, Ron Salemme, Marissa Chase) for making these past years an enjoyable experience and for their inputs to my research. Thanks to the intrepid John Green and Michelle Rolf for their valuable contributions on data collection (even on hazardous weather), laboratory analysis, and their friendship. Thanks to my everyday friends (Miriam Molina, Tito Lavaire, Dennis Pinto, Carmen Ugarte, Nuria Castañeda, Raúl Alfaro, and Frantz Obas) for their support, academic and personal advice, and encouragement. Thanks to the Zamorano community at UIUC for their friendship and good moments.

I deeply appreciate my parents and siblings for ALWAYS believing in me, supporting me, and for helping me even from a long distance. This goal could not have been possible without the patience, encouragement, understanding, help, support, and love of my wife and son, Helena and André, you have been my main motivation, los amo.

To Helena, André, mami, papi, Carlos, Ixchel, Celeste, Natalia, Ramiro, Sebastián, and Génesis.

Abuel@s Martha, Hilda, Adolfo, Tomás; Tí@s Rey, Santiago, Chila and Lita. L@s amo.

TABLE OF CONTENTS

CHAPTER 1: INTRODUCTION

Oxygen depletion zones in aquatic systems stem from anthropogenic interventions and have been spreading worldwide, especially in the Northern Hemisphere, since the mid– 1990s (Breitburg et al., 2018; Diaz and Rosenberg, 2008). Inputs of nutrients from point and diffuse sources not only increase nutrient availability but also alter the relative amounts of different types of nutrients in surface waters resulting in water quality impairment (Mekonnen and Hoekstra, 2018). In the United States, agriculture is the primary diffuse source of nutrient enrichment of surface water (Carpenter et al., 1998). Nutrient loadings from the Mississippi River Basin contribute to the emergence of algal blooms in the northern Gulf of Mexico, leading to the development of hypoxic areas (Turner and Rabalais, 2003). Attention to eutrophication in the Gulf of Mexico has recently increased, as the largest hypoxic zone ever recorded (22,730 km^2) occurred in 2017 since its measurement began in 1985 (NOAA, 2017).

Nitrogen (N) has historically been identified as the limiting nutrient for eutrophication in coastal-marine ecosystems. However, evidence suggests that reducing phosphorus (P) inputs to the Gulf of Mexico may minimize the adverse effects of algal growth (Alexander et al., 2007; Dodds, 2006; Howarth and Marino, 2006). Eutrophication in freshwater ecosystems is considered to be fundamentally regulated by P (Schindler et al., 2008) and co-limited by other elements (e.g., N and iron (Fe) (Sterner, 2008). In Lake Erie for example, the intensity of algal blooms is linked to P loads influenced by meteorological conditions and long-term trends in agricultural practices (Michalak et al., 2013; Smith et al., 2015b). The degradation of coastal-marine areas and freshwater resources has led to a focus on reducing P losses from agriculturally dominated landscapes (Mississippi River/Gulf of Mexico Watershed Nutrient Task Force 2008;

Ohio Phosphorus Task Force 2010) and necessitates investigation of the mechanisms and processes involved.

The factors involved in the loss of P are scale dependent, site specific, dynamic (Kleinman et al., 2011), and vary with the hydrology, geomorphology, meteorological conditions, and land use (Gelbrecht et al., 2005). The availability of P derived from these factors, along with the capacity to convey P from the soil to the outlet of the watershed is what determines P loadings (Fraterrigo and Downing, 2008). The two predominant transport pathways of P to streams in agricultural landscapes are surface runoff and subsurface flow (King et al., 2015b). The movement of P has long been associated with surface runoff because of P adsorption by eroded soil. As a result, P loading tends to be higher where overland runoff is the primary contributor to discharges (Blann et al., 2009). However, a combination of soil properties, climatic conditions, and management practices coupled with overfertilization can lead to the accumulation of significant levels of P in the subsoil, creating areas where P losses via subsurface flow are enhanced by tile (perforated pipes) drainage (Sims et al., 1998).

Artificial subsurface drainage is a widespread practice in agriculturally dominated landscapes of North America and Europe primarily. Although accurately assessing the extent of tile drainage is a difficult task as many tile lines were installed more than 50 years ago, it is estimated that 15.7 million ha are artificially drained in the midwestern US (Sugg, 2007). Subsurface drainage removes excess water from poorly drained soils providing aeration to root systems of crops and reducing ponding frequency, thereby increasing agricultural productivity. However, it may also increase P exports (Royer et al., 2006). Elevated concentrations of dissolved reactive phosphorus (DRP) have been reported in tile drainage water in east-central Illinois (Algoazany et al., 2007; Gentry et al., 2007; Xue et al., 1998) and Indiana, where 49% of

the DRP loading and 48% of the total P (TP) loading occurred through tile drainage (Smith, King et al., 2015). Yet studies reporting tile P loadings are relatively scarce. Additionally, factors contributing to P loss are incompletely understood, particularly in regions with a temperate climate (King et al., 2015b). Therefore, there is a need to further field-scale research on the factors influencing the transport of P in subsurface drainage in its multiple forms: DRP, particulate P (PP), and TP (Christianson et al., 2016).

Leaching of P in subsurface drainage systems can occur through the gradual interaction of water with the soil matrix and bypass flow via macropores that connect the soil surface to tile drains (Sims et al., 1998). Matrix flow can contribute the majority of water moving to tiles, but macropore flow has a significant potential to convey nutrients in fine-textured soils (Cullum, 2009). It is recognized that fine-textured soils have a higher sorption capacity than coarse-textured soils (Poirier et al., 2012); however, the tendency of fine-textured soils to create macropore flow conditions could be more influential to determine P losses than the sorption capacity. In Quebec, for example, the presence of subsurface drainage reduced losses of P from sandy loam soils, but increased losses from clay loam soils, which were considerably influenced by preferential flow (Eastman et al., 2010). Land management practices can progressively contribute to developing flow paths that rapidly convey water and constituents from the surface downward (e.g. preferential flow). Soil conservation tillage minimizes erosion and disturbance to preserve soil structure, yet enhancing subsurface P losses by developing macropores that increase vertical connectivity from the surface during wetting/drying cycles in fine-textured soils (Jarvis, 2007). In contrast, conventional tillage minimizes the risk of conveying chemical pollutants to subsurface drains by disrupting rapid preferential flow paths (Cullum, 2009). This explains why conventional tillage following fertilizer application resulted in lower P loads in

subsurface drainage water than conservation tillage during precipitation events in the non-growing season (NGS) in Ohio (Williams et al., 2016). The effectiveness of tillage to minimize the risk of losses from the P-enriched surface to tile drains is more evident when P fertilizer is incorporated into the soil (Djodjic et al., 2002; Williams et al., 2018). Similarly, crop residue in corn/soybean rotations under conservation tillage can promote tile P losses during thaw events (Messiga et al., 2010) due to the potential of freezing/thawing cycles to recreate macropores (Djodjic et al., 2002) and the crop residue capacity to leach DRP (Cermak et al., 2004; Ulén et al., 2010).

Landscape features (e.g., surface topography) produce variation in the hydrology and transport of nutrients and may also regulate P losses. Relatively flat landscapes derived from glacial till sustain highly productive row agriculture and are common throughout the Midwestern United States. Poorly drained soils and limited elevation differences have led to enhance soil trafficability during wet periods by installing artificial subsurface in this region, yet altering the hydrology and biogeochemical processes that result in nutrient enrichment of water bodies (Kalita et al., 2006; King et al., 2015a). Even flat agricultural landscapes contain closed depressions that have the capacity to store water for extended periods. At freezing temperatures, upper layers of the soil impermeabilize (Hayashi et al., 2003); therefore, the percolation capacity of the soil declines and its surface is prone to ponding conditions in closed topographic depressions. Under non-freezing conditions, prolonged ponding derived from reduced infiltration rates may occur when excessive rainfall raises the water level in the draining ditch and the outlet of the tile drains are submerged. These topographic features have the potential to alter hydrologic pathways and biogeochemical processes.

Improved understanding of DRP transport to tile drains is critical for determining the spatial distribution of critical source areas (CSA), that is, areas that disproportionately contribute to P loading at the watershed scale. Few studies have considered tile drainage effects on P loading when identifying CSAs, despite recognition that CSAs occur where pollutant sources coincide with active hydrologic transport mechanisms (Gburek et al., 2002; Sharpley et al., 2003; White et al., 2009). Mitigation actions are expected to be most effective in reducing watershed P loading when they target CSAs (Page et al., 2005). Improving the understanding of the mechanisms and processes involved in the DRP losses from surface soils of tile-drained fields and watersheds also contributes to identifying sustainable P management practices and targeting mitigation measures more effectively.

The goal of this research is to determine relationships among P losses, land surface topography, soil characteristics, management practices, meteorological conditions, and hydrologic characteristics on P losses in agricultural fields and watersheds dominated by tile-drainage in east-central Illinois. In Chapter 2, the specific objective is to evaluate how soil P and closed topographic depressions interact with precipitation and fertilizer application to affect tile DRP losses from a tile-drained field across seasons (i.e., growing and non-growing). In Chapter 3, the objective is to determine how preceding moisture conditions influence P losses from three agricultural watersheds in east-central Illinois and how the inclusion of antecedent water discharges improves the estimation of DRP and PP yields. Results from this research will improve understanding of the mechanisms and processes governing soil P loss in tile-drained fields and contribute to the design of more effective P management practices.

CHAPTER 2: CLOSED DEPRESSIONS AND SOIL PHOSPHORUS INFLUENCE SUBSURFACE PHOSPHORUS LOSSES IN A TILE-DRAINED FIELD

2.1 Introduction

Phosphorus (P) is an essential macronutrient for crop production and is routinely applied to corn and soybean fields. Phosphorus fertilizer readily binds to soil particles and has historically been considered an immobile soil nutrient subject to offsite transport via surface runoff and soil erosion (Sharpley et al., 1994). In relatively flat landscapes, especially in the Midwestern United States (US) and eastern Canada, poorly drained soils benefit from subsurface drainage (perforated pipes called tiles) to sustain highly productive row-crop agriculture (Fausey et al., 1995). However, evidence suggests that subsurface tile drains can transport substantial amounts of dissolved reactive P (DRP) to surface waters (Algoazany et al., 2007; Gentry et al., 2007; Smith et al., 2015a; Xue et al., 1998). Even relatively low loadings of bioavailable-dissolved P from diffuse sources raise the risk of environmental degradation because P is the limiting nutrient for eutrophication in freshwater ecosystems (Sharpley et al., 1994) and an important contributor to algal growth in coastal-marine ecosystems (Bierman et al., 1994). Although tile drainage is a beneficial practice, modifying the hydrologic regime by short-circuiting water transport has altered hydro-biogeochemical processes in ways that result in nutrient enrichment of water bodies (Kalita et al., 2006; King et al., 2015a).

A combination of factors drives the variability of subsurface P losses, including soil characteristics, the depth and spacing of drain tiles, management practices, hydrology, and meteorological conditions (King et al., 2015b; Sims et al., 1998). Although precipitation is the primary driver of P transport to tile drains (Gentry et al., 2007; King et al., 2015b; Pease et al., 2018; Van Esbroeck et al., 2017), the spatial heterogeneity of contributing sources challenges

the understanding of subsurface P losses. Soil test P (STP) has been shown to be positively related to tile DRP losses across fields (Duncan et al., 2017); however, this relationship and the spatial distribution of tile DRP losses at a sub-field scale is largely unknown. The spatial distribution of STP is influenced, in part, by contemporary and historical soil P surpluses (often termed 'legacies') that stem from past land use (e.g., livestock manure) and management practices that aim to build-up STP (Page et al., 2005). These legacies can mask the effect of other tile P loss drivers that are the subject of ongoing conservation efforts, thus delaying the intended improvement of water quality (Jarvie et al., 2013; Sharpley et al., 2013; Stackpoole et al., 2019).

The spatial variability of P in soils has also been associated with landform attributes due to sediment relocation from eroding to depositional positions (Quinton et al., 2010) and pedogenic processes (Letkeman et al., 1996). In flat agricultural landscapes in the Midwestern US, there are numerous closed topographic depressions that affect hydrology (Roth and Capel, 2012; Williams et al., 2019), biogeochemical processes (Smith et al., 2008; Suriyavirun et al., 2019), and land management practices (Feyereisen et al., 2015; Smith and Livingston, 2013). Conceptually, closed depressions are low-lying areas that are hydrologically disconnected to the overland runoff network, where ponding occurs when the intensity of rainfall surpasses the infiltration capacity or the water storage capacity of the soil. In flooded and anaerobic soils, mobilization via desorption and dissolution of precipitated P into the soluble-inorganic phase is well documented (Gu et al., 2017; Sallade and Sims, 1997; Shober and Sims, 2009; Young and Ross, 2001). In agricultural regions with closed depressions, previous research has identified P losses from low-lying areas that contain tile surface inlets designed to convey surface water directly to the subsurface drainage networks; therefore, bypassing the tortuous soil matrix (Ginting et al., 2000; Thoma et al., 2005; Tomer et al., 2010). Although these studies have

underlined the contributions of closed depressions to tile P losses via tile surface inlets, the role of closed depressions on P percolation to tile drains remains unclear. Investigating the effect of closed depressions on tile P losses in flat agricultural regions is pertinent because tile drainage designs often target low-lying areas to alleviate flooding conditions.

In this study, the overall goal was to improve understanding of factors that influence the seasonal and spatial variability of DRP losses from a tile-drained field. Specifically, the objectives were (i) to characterize the variability of tile DRP load and flow-weighted mean concentration (FWMC) across seasons (i.e., growing versus non-growing), and (ii) to investigate how STP (Bray P-1) and closed depressions interact with precipitation and fertilizer application to affect tile DRP loads and FWMC. Evaluating these drivers of P losses in flat tile-drained fields will improve the understanding of the sources of surface water quality impairment and can help inform decisions to optimize nutrient management efforts.

2.2 Methods

2.2.1 Site description

This study was conducted on a tile-drained field in Douglas County located in east-central Illinois (39º43′N, 88º14′W) (Fig. 2.1). The 30-year average precipitation at this site was 1008 mm based on measurements from the National Centers for Environmental Information (NCEI) weather station at Tuscola, IL (USC00118684) (NOAA, 2017), located 9 km NW from the study site. The study field is representative of the local topography with less than 2% slope. This region is dominated by extensive row-crop agriculture (corn/soybean rotation) with hydrology that has been substantially modified with dredged ditches that connect to existing rivers to convey drainage water from the fields. The predominant soils at the site are fine-textured, poorly drained, and classified as Milford silty clay loam (fine, mixed, superactive,

mesic Typic Endoaquolls)(USDA-NRCS, 2016). Approximately 40 years ago, a parallel drainage system was installed in the study field at depths ranging from 1.2 - 1.5 m below the soil surface and with a 30.5 m spacing. For this study, inline water level control structures (AgriDrain Corp., Adair, IA) were installed on 36 lateral tiles. On each instrumented tile, the respective monitoring structure was located approx. 4 m from the junction with the tile main that discharges to the ditch. The diameter of the tiles was 12.7 cm and the drainage area (plot size) ranged from 1.4 - 1.9 ha of cropland dependent on tile length (Appendix Table A1). The area drained by each instrumented tile is equivalent to the product of the drainage spacing and the length of the respective tile. None of the instrumented tiles had surface inlets.

2.2.2 Precipitation, tile discharge measurements, and water sampling and analysis

Cumulative daily precipitation was obtained from the NCEI weather station at Tuscola, IL (USC00118684) from Oct.1, 2014 through Jan 15, 2015 and was recorded at the study site from Jan 16, 2015 to Sep 30, 2017 using a weather station equipped with a tipping bucket rain gauge (Davis Instruments Corporation, Hayward, CA). Tile discharge rates were determined using a discharge equation for inline water level control structures developed by Chun and Cooke (2008). Each monitoring structure was equipped with a stoplog containing a 45º V-notch weir and water depth was recorded using a Water Level Datalogger Model 3001 (Solinst, Ontario, Canada) at 15-minute intervals.

From January 2015 to September 2017, water samples were collected from each of the 36 inline water level control structures using ISCO automated samplers (Teledyne Isco Inc., Lincoln, NE). Water samples were collected for analysis at 8-hour intervals during increased flow and weekly during base flow. Upon return to the laboratory, water samples were vacuum filtered through a 0.45 μm pore diameter membrane within 24 hours of collection from the tile

and stored at 4 ºC prior to analysis. Therefore, DRP is operationally defined as the <0.45 μm P fraction. Concentrations of DRP were determined colorimetrically with the ascorbic acid reaction method using a Lachat QuickChem 8000 FIA Automated Ion Analyzer (Hach Company, Loveland, CO). Dissolved reactive P concentrations between sampling times were estimated by linear interpolation. I computed DRP yields (kg ha^{-1}) by summing the product of continuous water discharge data and their corresponding interpolated DRP concentrations and dividing that sum (DRP load) by the drainage area of each tile. Annual tile yields and flow-weighted mean concentrations (FWMC) of DRP were calculated for each tile for each hydrological year (HY), defined as October 1st - September 30th. In HY 2015, DRP yields and FWMC from the first 3 months of the HY (Oct. to Dec. 2014) were not included in analysis because flow measurements began in January 2015. Here, the term 'DRP losses' is used to simultaneously refer to yields and FWMC of DRP. Water chemistry data for tile 33 were excluded from analysis in HY 2015 due to sediment contamination originating from the installation of the water level control structure; however, the contamination source was removed and data from tile 33 in HY 2016 and HY 2017 were included in the analysis.

2.2.3 Soil test phosphorus (STP) and topographic characteristics

In this study, soil cores were collected to a depth of 17 cm to quantify STP measured by the Bray P-1 method. Five soil cores were composited from a 30-cm radius circle centered at each sampling location. Depending on the length of an individual tile, composite soil cores were collected from a range of four to six locations spaced 100 m apart (2.5 acre grid) along each plot in November of 2016 (Fig. 2.1), and a mean STP concentration was calculated for each plot. Large individual STP concentrations in plots 33, 34, 35, and 36 (Fig. 2.1) led us to conduct

additional sampling along those plots in the spring of 2017, consisting of five composite soil cores from 22 sampling locations per plot with a 9.1 m spacing.

To characterize differences in STP with respect to the depth of depressions, additional sampling was conducted across two closed depressions in plots 1 (spring of 2017) and 16 (spring of 2018). These are the deepest closed depressions above monitored tiles in the study area. In each depression, five composite soil cores were collected to a depth of 17 cm from 45 locations distributed in three rows (15 locations per row) parallel to the tile. The rows were separated by 15.2 m from each other, and the spacing between sampling locations in each row was 9.1 m.

Surface terrain was characterized using 0.76-m square grid resolution (0.58-m^2 pixel) digital terrain models (DTMs) derived from light detection and ranging (LiDAR)(ISGS and IDOT, 2012). Depression depth (DD; meters) for each pixel was calculated as the difference between a hydrologically filled DTM (simulation of the water surface elevation in a completely inundated terrain) and the raw DTM (elevation of the terrain)(Planchon and Darboux, 2002). This approach produces accurate estimation of depression storage capacity (Amoah et al., 2012). To determine the depression depth integrated over the area drained by a tile, we computed a depression index (DI; m/ha) for each plot as

$$DI = \frac{\sum_{i=1}^{n} DD_i}{A} \quad (1)$$

where DD is the depression depth (m) for each pixel falling within the tile drainage area, and A is the corresponding tile drainage area (ha). All computations were done in ArcGIS v. 10.4.1 (ESRI, Redlands, CA).

2.2.4 Cropping system and management practices

A corn (*Zea mays* L.) and soybean (*Glycine max* L.) rotation system was grown during the study period on the farm. The field was divided into two sections with an equal number of

plots allocated to both crop phases every year (Appendix Table A1). The first section was comprised of plots 1 - 18, and the second was comprised of plots 19 – 36 (Fig. 2.1). Both sections of the farm were cultivated with corn during 2014, and in 2015, the first section began the rotation with corn and the second section with soybean. From 2015 through 2017, cumulative grain yields in the study farm compared to the Douglas County average were 1% greater for soybean and 8% lower for corn. During this period, the farm was the subject of an N timing study with a randomized complete block design. In April 2016, the second section of the farm (tiles 19 – 36) received surface-broadcasted inorganic P fertilizer at a rate of 103 kg P ha^{-1}. The commercial sources used were triple superphosphate (TSP) in plots 20, 23, 28, 32, and 36 and diammonium phosphate (DAP) in the remaining 13 fertilized tiles (Appendix Table A1). No P fertilizer was applied to tiles 1 – 18. During the study period, strip-till was performed during the fall (October – November) prior to the corn phase of the rotation, whereas soybeans were no-till planted. The growing season (GS) commenced with crop planting and ended the day of harvest. In all years, planting of both crops occurred in the last two weeks of May and corn harvesting from early to mid-October. Soybeans were harvested in late September, late October, and mid-October during 2015, 2016, and 2017, respectively. For this study, the 2015 non-growing season (NGS) began with the initial measured flow and DRP monitoring in January.

2.2.5 Data analysis

Linear mixed models (LMM) followed by Tukey's honestly significant difference (HSD) were used to quantify differences in average annual and seasonal (GS versus NGS) DRP yields and FWMC. The LMM captured temporal dependencies with year and season of sampling as fixed effects and tile ID as a random effect, fitted by the restricted maximum likelihood (REML) method in the nlme package (Pinhero et al., 2017). Linear regressions were performed to

examine the relationships among annual yields and FWMC of DRP, STP, and depression index. Dissolved reactive P data were log-transformed to meet assumptions of normality and equality of variance. Preliminary analysis of the relationship between STP and depression depth suggested a discontinuous function. Thus, I performed piecewise regression analysis using the Segmented Package (Muggeo, 2008) to identify the threshold at which the slope changed. The significance value in this study was set at 0.05. All the analyses were performed in the R statistical software v. 3.3.2 (R Core Development Team 2017).

Linear mixed models and an information theoretic approach (Burnham and Anderson, 1998) were used to assess the relative effects of soil test phosphorus, depression index, and their interaction with precipitation and phosphorus (P) fertilizer on tile dissolved reactive P losses at a monthly time step. Independent variables with a variance inflation factor (VIF) greater than three were sequentially excluded from the models until the VIFs remained below that threshold to reduce levels of multicollinearity. To allow direct comparison of the effect size of variables with different scales, all variables were standardized by subtracting the mean from each observation and dividing it by the standard deviation. Global models were fitted including all standardized predictors under investigation and the interactions among these terms specified as fixed effects, and tile ID as a random effect to account for temporal dependence. Models were compared to one another with the Akaike Information Criterion adjusted for small sample size (AICc) to assess goodness-of-fit. Model-averaged estimates (β) of the predictors were calculated from a subset of supported models with a cumulative AICc weight of 0.95 (Burnham and Anderson, 1998). The maximum likelihood (ML) function was employed because it allows direct comparison of models with different fixed effects. Model selection and estimate averaging were performed in the MuMIN package (Barton, 2016).

2.3 Results

Precipitation and its monthly distribution varied throughout the study period (Fig. 2.2). Total annual precipitation was greatest in HY 2016 (1069 mm), followed by HY 2015 (883 mm) and HY 2017 (870 mm). In 2015, precipitation was evenly distributed between the NGS (48%) and the GS (52%). A greater fraction of precipitation occurred during the NGS than during the GS in HY 2016 and HY 2017 (64% and 69%, respectively). The response of tile water discharge to precipitation differed seasonally (Fig. 2.2). During the GS, 16.1 ± 2.6% (mean ± SD), 8.6 ± 2.7%, and 15.5 ± 5.7% of cumulative precipitation were expressed as tile discharge in HY 2015, HY 2016, and HY 2017, respectively. The lowest monthly average flow and the least number of tiles actively flowing occurred during the GS, from July – October in 2015 and 2016, and from August - September 2017. In the NGS, the portion of rainfall expressed as tile discharge was 59.9 ± 11.0%, 37.8± 5.00%, and 46.8 ± 6.9% in HY 2015, HY 2016, and HY 2017, respectively.

Tile DRP losses exhibited both inter- and intra-annual variability (Fig. 2.2 and Table 2.1). Across all tiles, mean annual FWMC of DRP did not differ from HY 2015 (0.024 mg L^{-1}) to HY 2016 (0.023 mg L^{-1}; P=0.92) but increased to 0.033 mg L^{-1} in HY 2017 (P<0.01). Mean annual DRP yields significantly increased from 0.062 kg ha^{-1} in HY 2016 to 0.102 kg ha^{-1} in HY 2017 (P<0.01). Precipitation was positively related to DRP yield in both the GS and NGS, and to FWMC of DRP in the NGS (Table 2.2). Greater mean DRP yields occurred during the NGS in HY 2016 (90% of annual yields; P<0.01) and HY 2017 (92%; P<0.01) relative to their respective GS. Averaged FWMC of DRP was greater in the GS in HY 2015 (NGS: 0.016 vs. GS: 0.036 mg L^{-1}; P<0.01; Table 2.1), did not differ between periods in HY 2016 (NGS: 0.023 vs. GS: 0.020 mg L^{-1}; P=0.98), and was greater in the NGS in HY 2017 (NGS: 0.035 vs. GS: 0.018 mg L^{-1}; P<0.01).

Soil test P concentrations from individual locations across the study field ranged from 8 to 157 mg kg^{-1} (Fig. 2.1 and Appendix Fig. A1). Monthly FWMC of DRP and STP were positively associated in the NGS (Table 2.2), and at an annual scale, tile DRP yields increased with mean STP throughout the study with the strongest relationships in the last two years (Fig. 2.3). The greatest individual STP concentrations (61 - 157 mg kg^{-1}) occurred in the north section of the field, in areas overlying plots 33 – 36 (Appendix Fig. A1). Using a plat map and aerial imagery from the region, this area was later determined to be the location of a farmstead more than 70 years ago, which indicates the accumulated P in the soil derived from manure.

Monthly tile DRP losses increased with depression index in the NGS (Table 2.2). At the annual scale, the strength of the positive association between tile DRP losses and depression index was greatest in HY 2015 and declined in subsequent years. Across all plots, both annual yield (HY 2015: R^2=0.42; P<0.01; HY 2016: R^2=0.16; P=0.01) and FWMC of DRP (HY 2015: R^2=0.42; P<0.01 and HY 2016: R^2=0.10; P=0.04) were related to depression index in the first two years of the study, whereas in HY 2017 they were not significantly related (DRP yield: P=0.32, and FMWC: P=0.47). In contrast, positive relationships were found across all years between annual tile DRP yields and depression index where mean STP concentrations < 27 mg P kg^{-1} (Fig. 2.4), which is the concentration of sufficiency for optimal corn and soybean production in central Illinois (Fernández and Hoeft, 2009).

Relatively large STP concentrations coincided with the locations of closed depressions (Fig. 2.1). Consistently elevated yields and FWMC of DRP in tile 1, in contrast to adjacent tiles, led us to explore STP concentrations across the depression gradient (Fig. 2.5a). Piecewise linear regression demonstrated a critical threshold at a depression depth of 0.38 m at which STP concentrations increased (Fig. 2.5b). At depths greater than 0.38 m, a strong positive association

was observed between depression depth and STP (R^2=0.91). Soil sampling for the closed depressions in tile 16 (Fig. 2.5c) similarly demonstrated a threshold at a depression depth of 0.37 m, above which a positive relationship was observed (R^2=0.49; Fig. 2.5d).

In the NGS, DAP application interacted with depression index and precipitation to increase DRP yields and FWMC, respectively (Table 2.2). Similarly, increased DRP yields were related to TSP application in the NGS. Greater DRP concentrations were observed in tile water samples collected after P fertilization where DAP was applied than where TSP was applied or where no P fertilizer was used (Appendix Fig. A2). Although P was applied in the last month of the 2016 NGS, 51.4 ± 10.1% (mean ± SD) and 34.8 ± 2.7% of NGS DRP yields occurred after fertilization with DAP and TSP, respectively. In the same period, tiles with no P addition exported 22.8 ± 7.7% of that season's DRP yield.

2.4 Discussion

As expected, our results show that precipitation strongly affected tile DRP yields (Table 2.2). However, the magnitude of tile DRP yields in HY 2016 and HY 2017 was much greater in the NGS than the GS (Table 2.1), suggesting that crop water demand controls tile DRP losses by reducing discharge. Consistent with this interpretation, the greatest tile DRP yields were observed in the GS either early or late in the season, when plant water demand would have been relatively low (Fig. 2.2). Similar seasonal patterns in both tile water discharge and DRP yield have been documented previously in studies conducted in temperate regions with comparable precipitation regimes (Clement and Steinman, 2017; King et al., 2016; Van Esbroeck et al., 2016). These data highlight the importance of crops for attenuating precipitation-driven tile DRP losses and underscore the key role of the NGS for determining annual DRP losses from subsurface drainage.

The association between mean STP and annual tile DRP yields (Fig. 2.3) and the relative importance of STP for predicting monthly tile FWMC of DRP in the NGS (Table 2.2) indicate that P stored in the upper soil layer was delivered to subsurface waters. This relationship has been previously documented in hydrologically active arable soils (Duncan et al., 2017; McDowell and Sharpley, 2001). Moreover, tiles underlying areas with relatively large STP concentrations (tiles 33, 34, 35, and 36; Appendix Fig. A1) consistently ranked among the largest annual tile DRP yields since the beginning of the study (Appendix Table A2). Because these tiles drain an area where a farmstead was previously located (Appendix Fig. A1), this is interpreted as evidence that legacy P originating from manure drives elevated losses of DRP in subsurface drainage. Some individual STP concentrations in the area where the farmstead was previously located were up to fivefold greater than the amount needed for optimum corn and soybean production in central Illinois (27mg P kg^{-1}) (Fernández and Hoeft, 2009). Strategically withholding P applications to achieve agronomic optimum STP concentrations (Rowe et al., 2016) could potentially reduce the risk of legacy-derived DRP losses in subsurface drainage.

Closed depressions influenced both tile DRP yields and FWMC exclusively in the NGS (Table 2.2). This seasonal difference of the effect of closed depressions on DRP loss may result from greater evapotranspiration rates during the GS that reduce frequency and duration of ponding. The observed relationship between STP and depression depth beyond the threshold at 0.38 m suggests that the convergence of P-laden water and colloids from upslope positions carried with surface runoff lead to soil P accumulation in depressions (Fig. 2.5). Likewise, soil P accumulation in depressional areas was reported in a small agricultural watershed study in Manitoba, Canada (Wilson et al., 2016). Colloids deposited in depressions may become active sources of dissolved P given the increased potential of remobilizing particle-bound P in flooded

and saturated soils due to the microbially mediated reduction of Fe-oxyhydroxides (Gu et al., 2018; Henderson et al., 2012). Phosphorus solubilizing biological interactions and chemical reactions can also be affected by microbial community composition and soil characteristics across topographic gradients (Suriyavirun et al., 2019). These results are consistent with the detection of unusually high concentrations of soluble P in subsurface water from a plot near ponding-prone areas that coincided with the greatest topsoil P concentrations observed (50 mg P kg^{-1}) in a rotational cropping experiment in Iowa (Tomer and Liebman, 2014). Additionally, P may accumulate in closed depressions throughout the year with residual P losses expressed during the NGS. Anoxic conditions during critical stages of plant development may lead to reduced plant uptake of P, affecting corn (Jaynes et al., 2003) and soybean (Jaynes et al., 2005) yields compared to upslope areas, thereby attenuating depletion rates of the labile fraction of soil P in closed depressions. This is supported by previous research attributing the significant reduction of DRP concentrations in tile water in the NGS to increased crop uptake of P during the preceding GS in a continuous corn production system (Nash et al., 2014). Thus, while closed depressions disconnect the surface P transfer continuum at a watershed scale (Thomas et al., 2016), in tile-drained agricultural landscapes they may serve as P sources and delivery points hydrologically connected to the overland drainage network.

At the annual scale, positive effects of depression index on tile DRP yields were detectable only when mean STP concentrations were below the optimum for crop production in central Illinois (Fig. 2.4). The declining strength of this relationship across years may be explained by the dominant contributions of P derived from fertilization, especially in the NGS as evidenced by lower model-averaged parameter estimates for the depression index compared to DAP in the multivariate analysis (Table 2.2). The strong positive interaction between DAP and depression

index in the NGS (Table 2.2) and greater tile DRP concentrations from plots where DAP was applied (Appendix Fig. A2) further suggests that the direct exposure of highly soluble P fertilizer to ponding water immediately after application contributed to incidental tile DRP losses. In a study simulating rainfall on no-till plots, contact between broadcast soluble P fertilizer and ponding water resulted in highly concentrated DRP water, which was transported vertically through unsaturated and saturated preferential flow paths (Williams et al., 2018). Additional research involving isotope tracers may help determine the dominant transport mechanism of incidental losses in the study field.

High concentrations of accumulated residual soil P in low-lying areas indicate that these locations do not currently require additional P fertilizer. However, based on a typical 1 ha (2.5 acres) grid pattern used in soil mapping and fertilizer recommendations, sub-field scale hotspots may not be detected due to the variability in soil P concentrations across relatively small areas. I speculate that stratified sampling where a grid sampling scheme is supplemented with a targeted sampling of depressional areas may provide a more accurate characterization (i.e., soil mapping) of the field's soil P content (Mulla et al., 2000). This also suggests variable rate P fertilization would be beneficial in fields containing closed depressions to reduce P losses in tile drainage.

2.5 Conclusion

Dissolved reactive P exports from tile-drained fields encompass critical temporal and spatial components. Substantially greater tile DRP losses during the NGS underline the need to focus P management and loss reduction strategies to efficiently minimize the contributions of agricultural practices on water quality impairment in this period. Increased soil P concentrations associated with historical and recent management, and closed topographic depressions, can be important sources of tile DRP losses. This study's findings suggest the need to draw down soil P

in these areas to STP concentrations that do not exceed crop requirements. Soil sampling techniques that detect soil P variability at sub-field scales should be employed to accurately identify these locations to prevent soil P buildup and diminish the risk of soluble P exports from tile-drained fields while maintaining crop productivity.

2.6 Tables and Figures

Table 2.1. Mean seasonal yield and flow-weighted concentration of DRP of 36 tiles from hydrological years 2015 through 2017.

Hydrol. year	Season	DRP yield		FWMC of DRP	
		Mean (kg $ha^{-1)}$	Lower and upper bounds of 95% CI of the mean (kg ha^{-1})	Mean (mg L^{-1})	Lower and upper bounds of 95% CI of the mean (mg L^{-1})
2015	Non-growing	0.020	0.009 / 0.031	0.016	0.010 / 0.023
	Growing	0.025	0.015 / 0.036	0.036	0.029 / 0.042
2016	Non-growing	0.054	0.044 / 0.065	0.023	0.016 / 0.029
	Growing	0.006	-0.005 / 0.017	0.020	0.014 / 0.027
2017	Non-growing	0.094	0.084 / 0.105	0.035	0.029 / 0.042
	Growing	0.008	-0.002 / 0.019	0.018	0.011 / 0.024

Table 2.2. Model-averaged coefficient estimates for significant predictors and interactions for monthly tile DRP yield and FWMC in the growing and non-growing season. Underscored estimates denote significant predictors (conf. interval does not contain '0' for the respective season and response variable).

Parameter	Growing season		Non-growing season	
	β parameter estimate (DRP FWMC)	β parameter estimate (DRP yield)	β parameter estimate (DRP FWMC)	β parameter estimate (DRP yield)
Depression index	0.13	0.06	<u>0.19</u>	<u>0.12</u>
Precipitation	0.03	<u>0.54</u>	0.09	<u>0.41</u>
Soil test P	0.11	0.07	<u>0.27</u>	-
DAP	-0.13	0.02	<u>1.46</u>	<u>0.59</u>
TSP	0.13	-0.10	-	<u>0.49</u>
DAP * Depression index	0.07	-0.35	<u>1.26</u>	-
DAP * Precipitation	-	0.01	-	<u>0.21</u>

The reference level for fertilizer type (DAP and TSP) is "not fertilized". Coefficient estimates are based on scaled variables and thus reflect effect sizes.

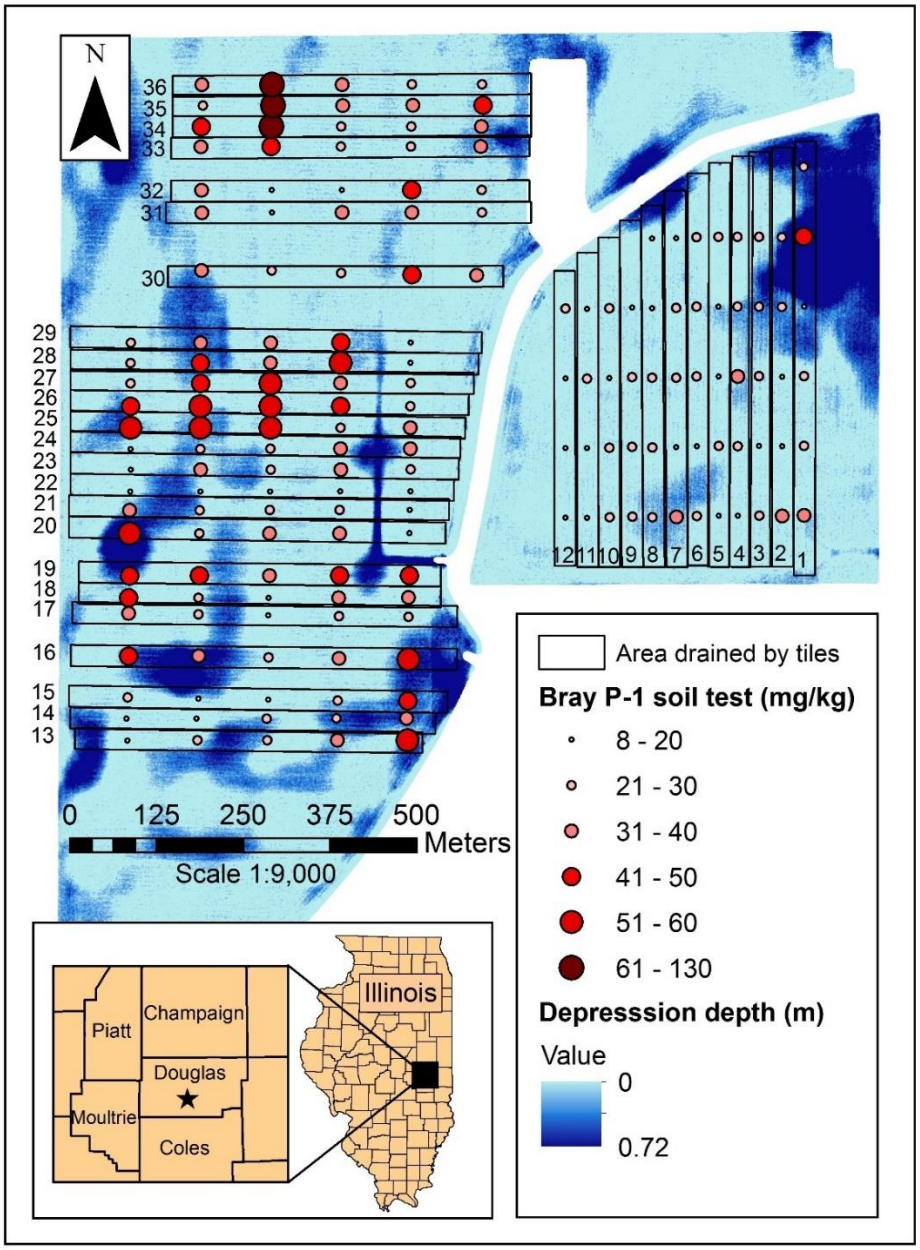

Figure 2.1. Depression depth, soil test P (STP) concentrations for each sampling location and distribution of the contributing area of 36 instrumented tiles.

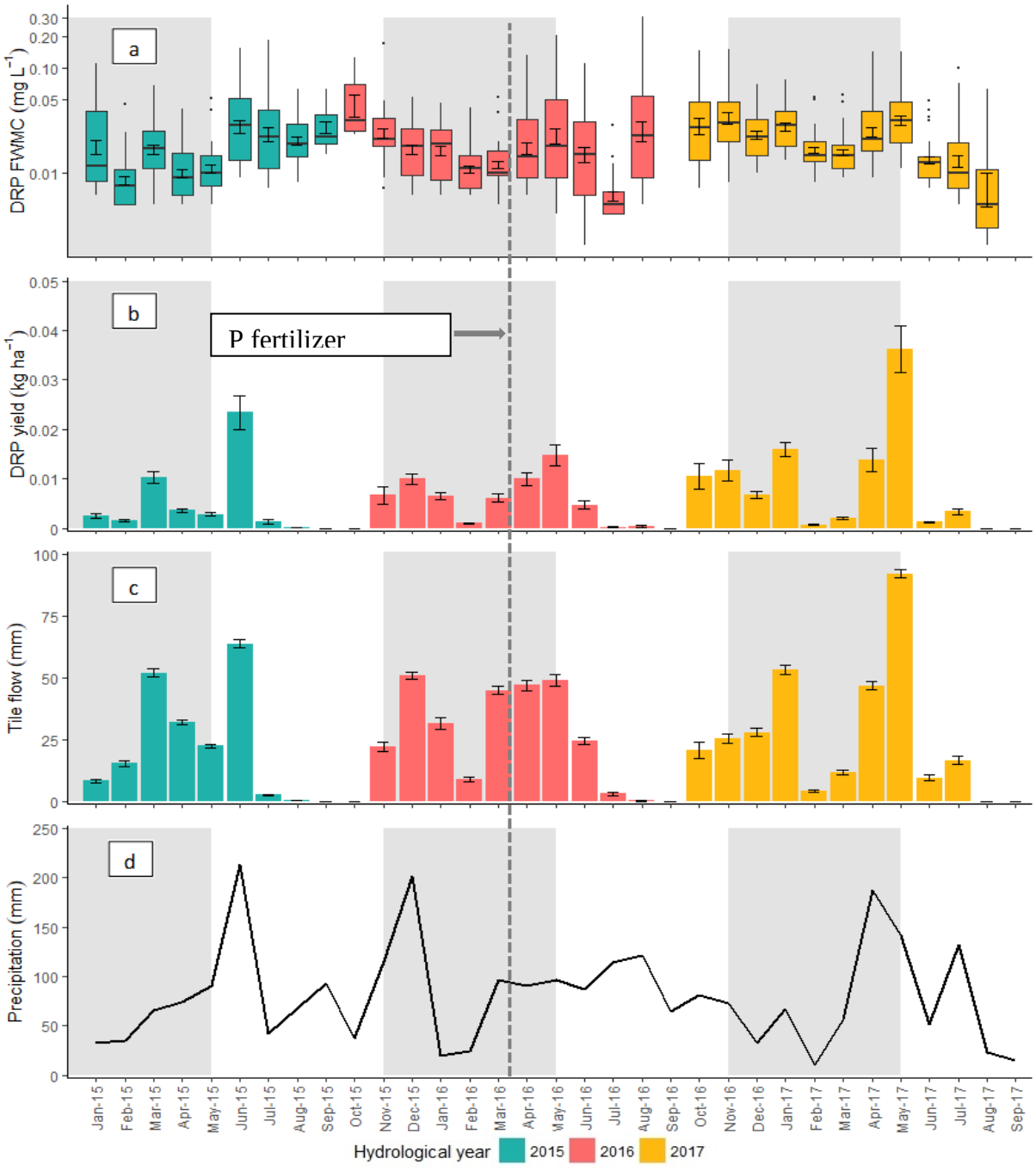

Figure 2.2. Monthly mean ± 1 SE of: A) flow-weighted mean concentration (FWMC) of tile DRP, B) tile DRP yield, and C) flow of 36 instrumented tiles. D) Cumulative monthly precipitation in the study site. Shaded periods depict non-growing seasons.

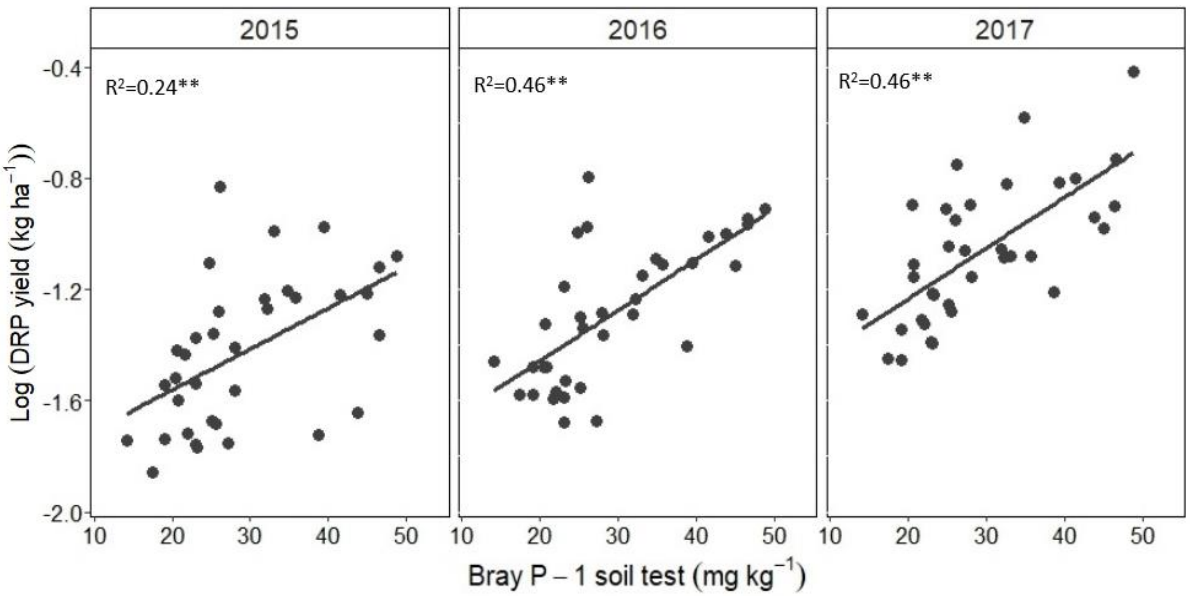

Figure 2.3. Relationship between log-annual DRP yield and mean soil test P (STP) concentration. ** P<0.01

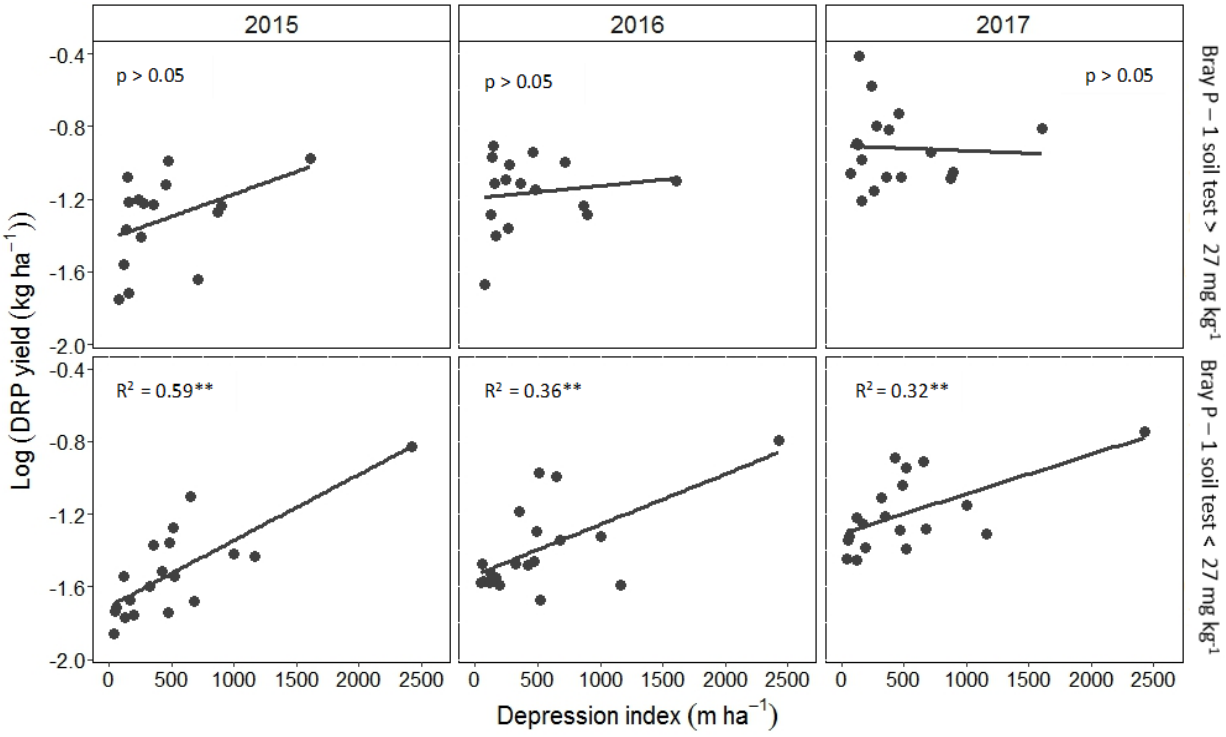

Figure 2.4. Relationship between log-annual DRP yield and depression index segregated by mean STP concentration at which yield does not depend on P additions to the soil. ** P<0.01

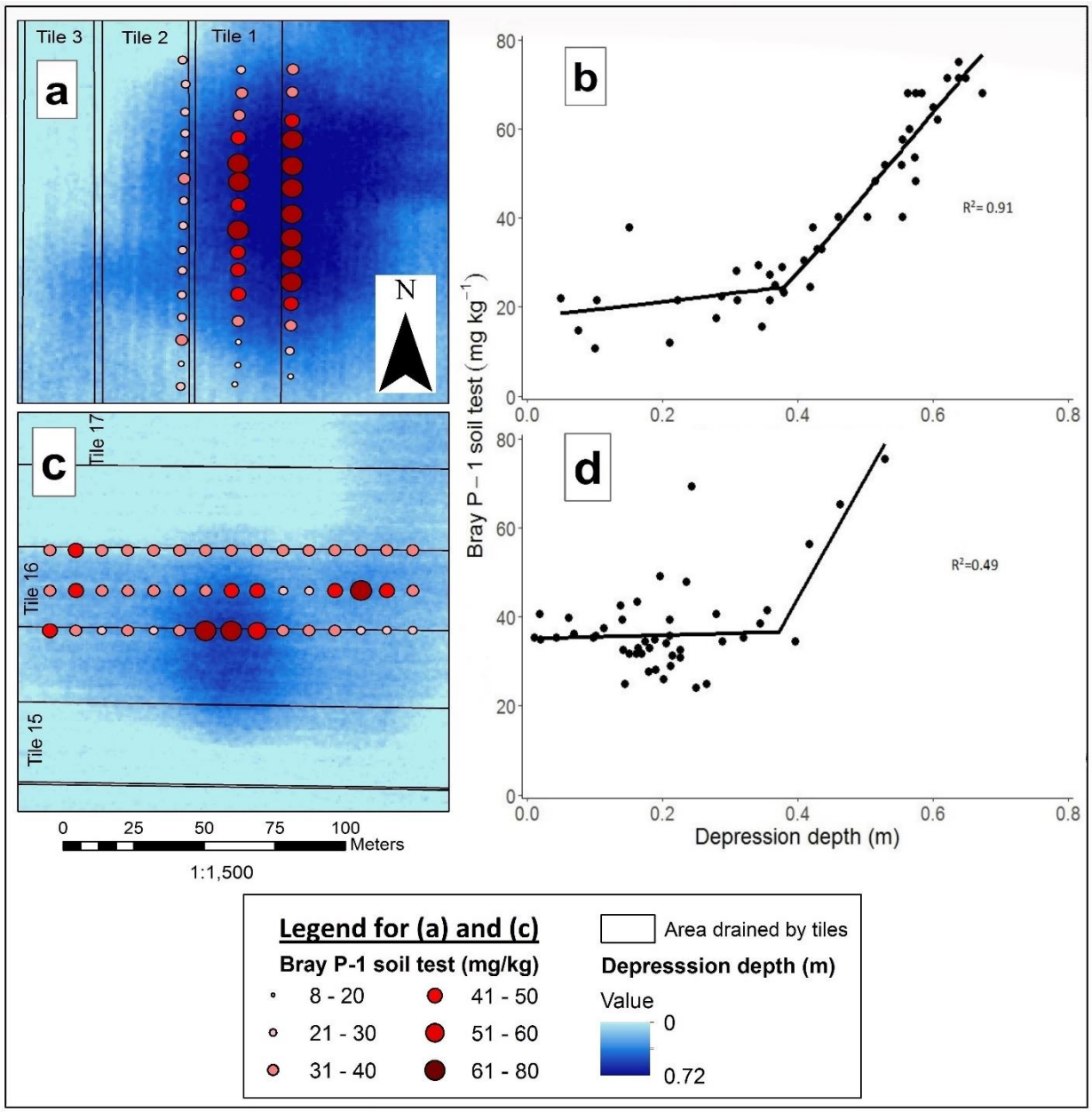

Figure 2.5. A) Soil test P (STP) concentration, depression depth, and B) their piecewise linear regression across closed depression in tile 1. C) Surface STP concentration, depression depth, and D) their piecewise linear regression across closed depression in tile 16.

CHAPTER 3: THE ROLE OF HYDROLOGIC DRIVERS ON PHOSPHORUS EXPORTS FROM AGRICULTURALLY DOMINATED WATERSHEDS

3.1 Introduction

Phosphorus (P) inputs from diffuse agricultural sources to downstream waters can degrade the quality of receiving aquatic ecosystems (Sharpley et al., 1994). In the Mississippi River Basin, agriculturally dominated watersheds have been identified as important contributors of P loads (Jacobson et al., 2011) that, coupled with nitrogen (N) loads, are the main sources of the hypoxic zone in the Gulf of Mexico (Turner and Rabalais, 2003). Phosphorus losses in agricultural watersheds derived from diffuse sources are not strictly related to inputs on a short time scale (e.g., fertilizer application) (Jacobson et al., 2011). Instead, a P 'spiraling' (continuous transfers among the soil, water, and biota phases) may delay exports of surplus P to downstream waters, increasing the complexity to maintain a balanced P cycling and to implement P loss reduction practices (Sharpley et al., 2013). Management of P exports from agricultural watersheds has been traditionally based on the Critical Source Area (CSA) framework (Pionke et al., 2000; White et al., 2009). These areas are defined as locations where P sources or 'hotspots' and enhanced hydrological connectivity to the stream network intersect, resulting in greater risk of P movement to streams. Although this approach is based on reliable evidence and has resulted in substantial advances to strategically target and prioritize mitigation measures, there are multiple components that interact with P sources and transport capacity to determine the risk of pollution of aquatic ecosystems. For instance, the buffering capacity of a watershed (ability to resist changes on P concentrations and loads in surface waters) encompass geochemical, hydrological, and biomass storage components that modulate the effects of known P loss drivers (e.g., P legacies and precipitation) (Doody et al., 2016).

Antecedent moisture conditions can be an indicator of the buffering capacity of a watershed by determining constituent and water exports based on historical records because moisture conditions influence source availability and the activation of transport mechanisms (McMillan et al., 2018). Although precipitation is the main control of flow generation in tile drains, antecedent moisture conditions mediate the runoff-to-precipitation response during bare soil periods and early stages of the growing season, when nutrient losses are more likely to occur (Vidon and Cuadra, 2010). Surface runoff generation and the potential to transport sediment-bound P increases with greater soil moisture content (McDowell and Sharpley, 2002). However, the effect of antecedent moisture conditions on nutrient dynamics has been studied primarily for nitrogen losses (Davis et al., 2014; Vidon et al., 2009). Additionally, improving our understanding of the relationship between nutrient losses and antecedent moisture conditions requires long-term datasets of constituent concentrations which in many cases are not readily available.

Several models and statistical tools have been developed to simulate and estimate P loads and P conveyance to streams at a range of spatial scales. The applicability of statistical and process-based models is determined by the extent and resolution of available data, processes involved, and objectives of the researchers (Baffaut et al., 2015). The Weighted Regressions on Time, Discharge, and Season (WRTDS) is a statistical technique that uses as explanatory variables time of the year, daily discharge, and seasonal trends to estimate constituent loads at a daily time-step (Hirsch et al., 2010). To obtain an accurate estimation of constituent loads, Zhang and Ball (2017) included antecedent discharge anomalies as an explanatory variable. However, the authors recognize that further studies should be performed to identify the areas for improvement of this statistical method.

In this study, the overall objective is to improve our understanding on how antecedent hydrologic conditions affect dissolve reactive P (DRP) and particulate P (PP) exports from agricultural watersheds dominated by tile drainage. Specifically, I i) evaluated how hydrologic drivers (precipitation, water retention capacity, runoff, baseflow) affect P exports and, ii) assessed the performance of the WRTDS method to estimate P exports with and without the inclusion of an antecedent flow anomaly term.

3.2 Methods

3.2.1 Study region

This study was conducted using data from three agriculturally dominated watersheds within the Mississippi River Basin located in east-central Illinois. The watershed outlets are defined by the location of gauging stations monitored by the United States Geological Survey (USGS) (Fig. 3.1). The topography is predominantly flat with slopes less than 2% derived from the Wisconsin glaciation. More than 90% of the land is used for row crop agriculture, mainly under a corn (*Zea mays* L.) and soybean (*Glycine max* L.) rotation and scarce animal production (David et al., 2016). The predominant soils are fine-textured and classified as Drummer silty clay loam (fine-silty, mixed, superactive, mesic Typic Endoaquolls) and Flanagan silt loam (fine, smectitic, mesic Aquic Argiudolls) (USDA-NRCS, 2016). Artificial subsurface (tile) drainage is prevalent in the region to accelerate excess water removal from poorly drained soils to benefit row crop production. However, tile drainage has altered the hydrologic and biogeochemical dynamics of the region by increasing hydrological connectivity and contributing to N and P exports to downstream water bodies (Royer et al., 2006).

The upper Embarras River (EMC) watershed is delimited by USGS site 03343400 near Camargo, IL draining 481 km^2 mostly distributed between Champaign County and Douglas

County. The EMC watershed receives an average discharge of 0.21 mega gallons per day (Mg d^{-1}) from the sewage treatment plant of Villa Grove, IL. The Lake Fork of the Kaskaskia River (LFK) watershed (386 km^2) is delimited by the USGS site 05590800 near Atwood, Piatt County and is primarily located in Piatt and Champaign County. The Salt Fork (SF) watershed drains 347 km^2 in Champaign Co. and is monitored by the USGS site 03336900 near St. Joseph. The Rantoul sewage treatment plant delivers an average of 2.81 Mg d^{-1} of water to the SF river. These three watersheds are representative of topographic characteristics and agricultural practices of east-central Illinois.

3.2.2 Precipitation, discharge measurements, and water sampling and analysis

Cumulative daily precipitation records were obtained from the National Centers for Environmental Information weather station network (NOAA, 2017) at EMC (Villa Grove 0.6 ESE, Broadlands 0.1 SSW, Willard Airport, Philo, and Rantoul), LFK (Monticello 3.5 NNE, Atwood 0.4 N, Atwood 5.4 NW, Hammond, Tuscola), and SF (St. Joseph 0.6 NE, St. Joseph 0.9 SSW, Thomasboro 5.2 E, and Rantoul). For each watershed, cumulative daily precipitation was calculated as the average daily values across all the corresponding weather stations. Measured discharge records were obtained from the USGS gauge site at the watershed outlets.

Water samples were collected at the outlet of the watersheds on a weekly basis since June 1993 (EMC), October 1996 (LFK), and March 2010 (SF) through September 2018. After collection, water samples were processed and stored as described in Chapter 2. Dissolved reactive P was determined colorimetrically using a spectrophotometer until November 2002 and using the ascorbic reduction method with a Lachat QuickChem 8000 FIA Automated Ion Analyzer (Hach Company, Loveland, CO) from December 2002 through the end of the study as described in Chapter 2. Total P (TP) was determined from unfiltered water samples and digested

with ammonium persulfate and sulfuric acid. Operationally defined particulate P (PP) was calculated as the difference between TP and DRP. Annual yields and flow-weighted mean concentrations (FWMC) of DRP and PP were obtained by linear interpolation as described in Chapter 2. Annual runoff was determined by dividing annual discharge by the watershed area. In this chapter, all years are based on the hydrological cycle (October 1st - September 30th) instead of the calendar year.

3.2.3 Data analysis and the weighted regressions on time, discharge, and season method

Linear regressions were used to evaluate bivariate relationships using a significance level of 0.05 and were performed in the R statistical software v. 3.3.2 (R Core Development Team 2017). In this study, river runoff was used as a proxy for moisture conditions (Murphy et al., 2014; Zhang and Ball, 2017) and the runoff-to-precipitation ratio (R:P) as a proxy for water retention capacity in the watershed (Goyette et al., 2018a). Power law relationships were employed to characterize the response of DRP and PP concentrations to discharge and are defined as

$$Y = aQ^b \quad (2)$$

where Y is the daily nutrient yield (area-weighted load), a is the intercept, Q is the discharge, and b is the slope (elasticity coefficient). Increments in discharge can result in dilution or dominant baseflow (b<1), invariable concentrations (b=1), or increased concentrations (b>1). Particulate P yields from LFK for 2012 and from EMC for 2000 were excluded from the power law analysis due to an excessive number of zeroes in the dataset. Across three watersheds, about 75% of total water discharge occurred when daily discharge >1 mm day^{-1} during the study period; therefore, baseflow was defined as daily discharge <1 mm day^{-1} equivalent to 5.6 m^3 s^{-1} at EMC, 4.46 m^3 s^{-1} at LFK, and 4.0 m^3 s^{-1} at SF.

The evaluation of the base WRTDS and the modified version (with the inclusion of the antecedent flow anomaly term) is based on Zhang and Ball (2017). An antecedent flow anomaly (AFA) term was added to the base model proposed by Hirsch et al. (2010) in the EGRET package in R. The modified equation for WRDTS is

$$\ln(C) = \beta_0 + \beta_1 t + \beta_2 \ln(Q) + \beta_3 \sin(2\pi t) + \beta_4 \cos(2\pi t) + \beta_5 \text{AFA} + \varepsilon \quad (3)$$

where C is concentration, t is time in decimal years, Q is discharge, β is the parameter coefficient, AFA is the antecedent flow anomaly and ε is the error term. The estimated concentrations and loads generated by the base and modified WRTDS models were evaluated against observed data using a modified Nash-Sutcliffe efficiency coefficient (E). The different AFA terms (equations 4 - 16) and the formula of E (equation 15) are described in Appendix B1.

3.3 Results

3.3.1 Hydrologic drivers of P losses

Average annual precipitation was 973 mm at EMC (1994 – 2018), 1015 mm at LFK (1997 – 2018), and 1016 mm at SF (2008 – 2018) (Appendix Table B1). During the first period of the study (1994 – 2007 for EMC and 1998 – 2007 for LFK), average annual precipitation was 4.9% and 6.4% lower than the average annual precipitation of the entire study period at EMC and LFK, respectively. Whereas, during the second period (2008 – 2018), average annual precipitation was 5.6% and 5.7% higher than the average at EMC and LFK, respectively. Across all three watersheds, 2008 was the wettest year followed by 2016 and 2010, and for EMC and LFK, 2002 was the fourth wettest year. The driest years were 2000 (676 mm), 2012 (734 mm), and 2013 (868 mm) for EMC, LFK, and SF, respectively. During the period of record for each watershed, the area-weighted water discharge (runoff) ranged from 676 – 1289 mm at EMC, 735 – 1481 mm at LFK, and 868 – 1411 mm at SF. Runoff was related to summed annual

precipitation at EMC (R^2= 0.38; P<0.01) and LFK (R^2=0.56; P<0.01), but not at SF (P=0.21) (Appendix Fig. B1). As expected, the proportion of precipitation that became river runoff, expressed as the runoff to precipitation ratio (R:P), was strongly related to runoff (R^2 greater than 0.85 and P<0.01 for all three watersheds) (Appendix Fig. B1). Mean R:P ratio over the period of record was 0.33, 0.29, and 0.34 at EMC, LFK, and SF respectively.

Both annual DRP and PP yields varied across watersheds and years; however, annual PP yields were more variable than DRP yields throughout the study period (Appendix Table B1). Average annual DRP yields were 0.47 ± 0.24 kg P ha^{-1} (mean ± SD), 0.34 ± 0.24 kg P ha^{-1}, and 0.50 ± 0.14 kg P ha^{-1} at EMC, LFK, and SF, respectively. Whereas, average annual PP yields were 0.42 ± 0.36 kg P ha^{-1}, 0.36 ± 0.33 kg P ha^{-1}, and 0.39 ± 0.19 kg P ha^{-1} at EMC, LFK, and SF, respectively. Both DRP and PP annual yields were positively related to precipitation at EMC and LFK (Appendix Fig. B2) and to R:P ratio (marginally significant for PP yields at SF; P=0.08). At SF, this association was marginally significant for DRP (P=0.06) and not significant for PP (P=0.27). Dissolved reactive P: Total P ratios varied temporally and across watersheds. During the study period, average daily DRP:TP concentration ratios were lower than 0.5 at LFK, with the exception of 1998 (Appendix Fig. B3). At SF, average daily DRP:TP concentration ratios were greater than 0.5 across all years; however, during the 2009 – 2014 period, this ratio ranged between 0.70 and 0.81, and during 2015 – 2018 ranged from 0.52 to 0.62. When excluding baseflow data (runoff <1 mm day^{-1}), DRP:TP increased and showed greater inter-annual variability at LFK (Fig. 3.2), remained above 0.5 at SF, and was negatively related to annual precipitation (R^2=0.28; P=0.01) at EMC (Fig. 3.5). The non-baseflow runoff fraction (> 1 mm day^{-1}) represents nearly 70% of total runoff in all three watersheds. On average, the non-

baseflow fractions of total annual DRP and PP yields were 89 and 83% at EMC, 86 and 81% at LFK, and 74 and 83% at SF, respectively.

The positive relationship between annual precipitation and elasticity coefficient (b) was significant for PP yields at EMC (R^2=0.21; P=0.03) and marginally significant at SF (R^2=0.32; P=0.09) (Fig. 3.4). Elasticity coefficient (b) increased after the area-weighted baseflow data (< 1 mm of discharge per day) were excluded from analysis (Appendix Table B2). For DRP yields, average elasticity coefficient (b; unitless) increased after excluding baseflow data from 0.99 ± 0.11 to 1.89 ± 0.26 at EMC, from 1.00 ± 0.17 to 2.00 ± 0.27 at LFK, and from 0.97 ± 0.42 to 1.44 ± 0.20 at SF. At the latter watershed and before excluding the baseflow data, the average slope (b) of the 2009 – 2014 period was notably lower (0.64 ± 0.14) than that of the 2015 – 2018 period (1.47 ± 0.06). Average elasticity coefficient for PP yield was also greater when the baseflow data were excluded, which changed from 1.07 ± 0.16 to 1.70 ± 0.32, from 0.88 ± 0.13 to 1.77 ± 0.30, and from 1.19 ± 0.26 to 1.60 ± 0.28 at EMC, LFK, and SF, respectively. Elasticity coefficient for PP and DRP yields were not related to precipitation when the baseflow data were excluded.

3.3.2 WRDTS and the inclusion of antecedent flow anomalies

The performance of the base WRTDS model in relation to observed data varied across watersheds and P fractions (DRP and PP) (Table 3.1). The coefficient of determination (R^2) between observed annual DRP loads and those calculated by the base WRTDS were 0.85 at EMC, 0.75 at LFK, and 0.65 at SF. Likewise, for PP yields the R^2 was 0.59, 0.84, and 0.62 at EMC, LFK, and SF, respectively. For both P fractions and all watersheds, load calculations performed better than concentrations. The inclusion of the antecedent flow anomaly term to the base WRTDS model maintained or, in few cases, modestly increased the E-values for both DRP

and PP relative to the base WRTDS model (Table 3.1). Although small, improvements based on the E-value were consistent with the addition of the average discounted flow (ADF) term for both P fractions and across all three watersheds. The R^2 of DRP and PP yields across the 12 modified and base WRTDS models indicated the years with greater inconsistency among the tested models. At EMC, the years 2000 for DRP yields and 1996 for PP yields showed the highest variability across models; whereas at LFK, 2012 for DRP yields and 2003 for PP yields exhibited the greatest variability. At SF, that year was 2012 for both DRP and PP yields.

3.4 Discussion

Results from this study indicate that not all the hydrological responses to precipitation were uniform, even though all three monitored watersheds were largely dominated by row crop agriculture (85 – 90%). Similar to previous studies conducted in artificially drained watersheds (King et al., 2015a; Macrae et al., 2007), annual precipitation was related to runoff at EMC and LFK (Appendix Fig. B1). However, runoff was disproportionately reduced at SF during the 2012 drought, affecting the runoff-to-precipitation (R:P) response. Although 2012 was not the year with the lowest cumulative precipitation during the period of record at SF, 35% of the total precipitation occurred in the last two months of that hydrological year when crop water demand and evapotranspiration rates were high. At all sites, the R:P ratio, interpreted as the percentage of precipitation that resulted in river discharge at the watershed outlet, was a stronger predictor of runoff than cumulative precipitation (Appendix Fig. B1). Mean R:P ratio at the study watersheds were lower than those recorded in 18 agricultural watersheds in Quebec, Canada (Goyette et al., 2018b). Despite the prevalence of tile drainage in the study watersheds, low R:P ratios suggest higher water retention capacity probably due to topographic characteristics (e.g., lower slopes, closed topographic depressions) and predominant fine-textured soils.

The positive relationship between both DRP and PP yields with R:P ratio likely originated from the response of runoff to R:P ratio, indicating that years with lower water retention capacity (high R:P ratio) exhibited greater P downstream transfer (Fig. 3.3). In this study, the water retention capacity of the monitored watersheds acted as a buffer of the effect of precipitation on DRP and PP exports. Previous work has examined the effect of R:P ratio on P loads in areas dominated by tile drainage. For example, R:P was related to greater N and P exports (quantified as the fraction of constituent losses relative to net anthropogenic inputs) in Québec, Canada (Goyette et al., 2018a). In Ohio, DRP and TP loads increased with R:P ratio in fields with lower soil test P concentrations, and at R:P<0.2, subsurface TP loading met the recommended target for the Lake Erie (<1.24 kg ha^{-1}) with soil test P (Mehlich III) of 125 mg kg^{-1} (King et al., 2018).

Annual PP yields were more variable than DRP yields (Appendix Table B1) due to the episodic nature of erosional processes (Heathwaite et al., 2005). With a 23 year-record, the relationship between precipitation and daily average DRP:TP ratio when runoff > 1mm day^{-1} (non-baseflow fraction) at EMC (Fig. 3.5) supports the interpretation made by Royer et al. (2006) and Gentry et al. (2007) that wet years result in greater proportion of PP losses relative to DRP (low DRP:TP). In Iowa, large variability of DRP:TP ratios observed in 12 agricultural watersheds (Range: 0.08 – 0.68) were associated with crop intensity and with important contributions of baseflow (Schilling et al., 2017). Additionally, the association between the elasticity coefficient "b" with precipitation at EMC and SF indicates that PP exponentially increases with precipitation. These findings suggest that during wet years, the probability of soil saturation, surface runoff generation, and sediment-bound P transport increases, thus, activating the hydrological connectivity of the watershed.

Dissolved reactive P to total P (DRP:TP) ratios at SF were highly influenced by discharges of the City of Rantoul sewage treatment plant that delivered to the SF River an average of 0.45 Mg P $year^{-1}$ (Fig. 3.2). In 2014, the Rantoul sewage treatment plant began the removal of soluble P which explains the reduction of DRP:TP ration in the subsequent years (Fig. 3.2). The effect of sewage effluent was also observed on the elasticity coefficient at SF for DRP from 2009 to 2014 (Appendix Table B2) which abruptly increased in 2015 after P removal was implemented. The influence of the Villa Grove sewage treatment plant was not as evident for EMC as the Rantoul plant for SF, probably because the Villa Grove plant delivers an average of 0.21 Mg of water d^{-1} compared to 2.81 Mg d^{-1} delivered by the Rantoul plant. Both, the DRP:TP ratio and the elasticity coefficient were calculated based on daily values; therefore, baseflow conditions had the same weight as days with greater P loads (e.g., precipitation events, snowmelt). Despite the influence that baseflow can exert on the interpretation of these analyses, low flow only contributed from 11 to 26% of the annual P loads. Special attention should be given when investigating the behavior of water quality constituents, especially P, because baseflow conditions may control hydrologic and biogeochemical responses at a daily scale that do not necessarily reflect the potential effect on nutrient loadings.

The performance of the base and modified WRTDS models, with respect to observed data, was watershed and P fraction dependent (Table 3.1). The base and modified WRTDS models at EMC produced greater E-values compared to LKS and SF which can be, in part, related to the flashy responses of discharge to precipitation at the latter watersheds (Hirsch et al., 2010). Particularly at SF, water discharge can increase an order of magnitude within 24 hours from the onset of the event. Increasing the frequency of the time-step (e.g., 0.5 or 0.33 days) at these watersheds could potentially alleviate this problem. The inclusion of the antecedent

discharge anomaly term into WRTDS did not substantially increase the performance of the model. E-values were consistent with those of the base model, suggesting that improvements of the modified models were likely an effect of the base model.

Findings from this study support the interpretation made by Zhang and Ball (2017) that the lack of substantial improvement of the modified WRTDS models to estimate DRP exports can be attributed to physico-chemical and biological processes occurring in the watersheds (Zhang and Ball, 2017). Linear regressions between observed and WRTDS-derived nutrient loads allowed to identify 'outlier years'. At all three watersheds, WRTDS underestimated DRP concentrations and loads in February 2007 and February 2014, years that experience snowmelts with a substantial amount of fertilizer as suggested by the greater proportion of DRP losses in relation to TP (Appendix Fig B4). At EMC, those events accounted for 64% of the annual DRP load in 2017 and 54% in 2014. Interestingly, WRTDS estimated greater PP concentrations and loads than those observed in 1996 at EMC. After a detailed exploration of the dataset, it was noted that under the sampling frequency at that moment (biweekly) two precipitation events that substantially increased runoff were not sampled. In this case, the observed concentrations differed from the WRTDS estimations because the sampling frequency resulted in an underrepresentation of reality.

3.5 Conclusion

Results from this study suggest that the water retention capacity (R:P) of a watershed buffers the effect of precipitation on P exports. In agricultural watersheds, timing, frequency, and intensity of precipitation can affect hydrological responses that alter the transport capacity of nutrients and pollutants. Thus, hydrologic connectivity is not necessarily a constant over time and varies depending on watershed characteristics. The response of P exports to precipitation can

vary depending on crop water demand, evapotranspiration, soil saturation, precipitation intensity, infiltration capacity, topographic variations, and soil type. These variables may act differently on both fractions of P (DRP and PP); therefore, the DRP:TP ratio could be a good indicator to define water quality goals and prioritize mitigation measures.

Due to a wide range of drivers, predicting the transport of P in tile-drained watersheds is complex. At this moment, even in relatively homogeneous watersheds (e.g., similar topography, agricultural practices, soil type) the performance of statistical tools and process-based models that estimate and predict P transport need improvement. Improving the prediction of P transport for different fractions and not only TP is also important because they result in different implications for water quality. However, this is a challenging task that will require better understanding of hydrologic drivers of P movement due to the contributions of DRP from tile drainage and the episodic nature of PP on intensively cultivated landscapes.

3.6 Table and Figures

Table 3.1. Performance of the base and proposed models relative to observed concentrations and loads.

Method	Embarras (EMC)				Lake Fork - Kaskaskia (LFK)				Salt Fork (SF)			
	DRP		PP		DRP		PP		DRP		PP	
	Conc.	Load	Conc.	Load	Conc.	Load	Conc.	Load	Conc.	Load	Conc.	Load
	----------E (Modified Nash-Sutcliffe Efficiency)----------											
WRTDS	0.51	0.80	0.32	0.65	0.39	0.69	0.31	0.62	0.36	0.79	0.32	0.71
WRTDS + LTFA	0.51	0.80	0.33	0.67	0.38	0.69	0.35	0.65	0.36	0.78	0.33	0.73
WRTDS + MTFA	0.53	0.81	0.32	0.64	0.40	0.70	0.32	0.62	0.35	0.80	0.34	0.72
WRTDS + STFA	0.54	0.81	0.33	0.65	0.39	0.70	0.33	0.64	0.38	0.80	0.34	0.72
WRTDS + AnnualFA	0.51	0.80	0.33	0.66	0.38	0.69	0.35	0.65	0.38	0.78	0.33	0.73
WRTDS + SeasonFA	0.52	0.80	0.32	0.64	0.40	0.70	0.33	0.63	0.35	0.79	0.33	0.71
WRTDS + DailyFA	0.52	0.80	0.33	0.65	0.40	0.70	0.36	0.67	0.36	0.79	0.33	0.73
WRTDS + FA100	0.52	0.80	0.33	0.65	0.40	0.71	0.36	0.67	0.35	0.79	0.33	0.73
WRTDS + FA10	0.53	0.81	0.33	0.65	0.39	0.69	0.32	0.62	0.35	0.81	0.34	0.72
WRTDS + FA1	0.54	0.81	0.35	0.65	0.39	0.70	0.34	0.66	0.39	0.80	0.35	0.72
WRTDS + ADF	0.55	0.82	0.35	0.66	0.41	0.70	0.35	0.65	0.39	0.82	0.34	0.72
WRTDS + dQ/dt	0.53	0.80	0.36	0.63	0.39	0.69	0.33	0.64	0.37	0.80	0.37	0.73
WRTDS + BFI	0.55	0.81	0.34	0.64	0.37	0.70	0.33	0.65	0.37	0.79	0.34	0.72

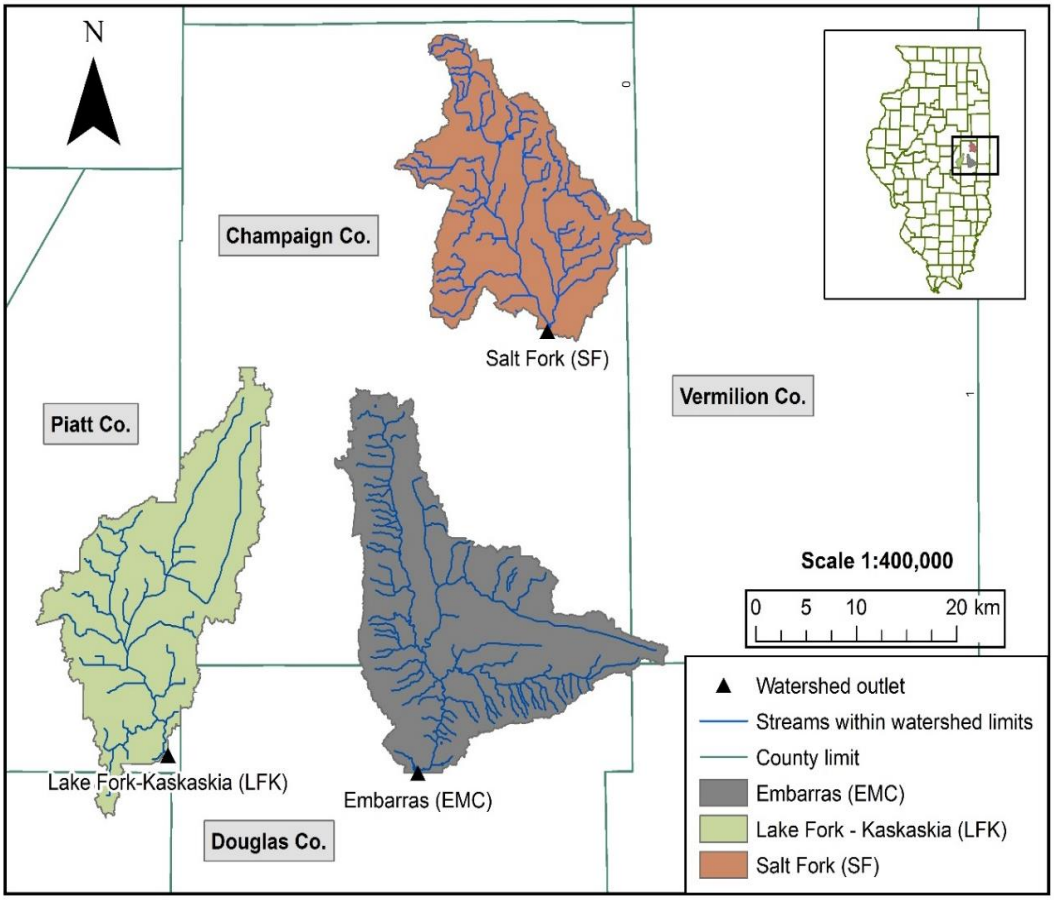

Figure 3.1. Location of the three monitored agricultural watersheds in east-central Illinois.

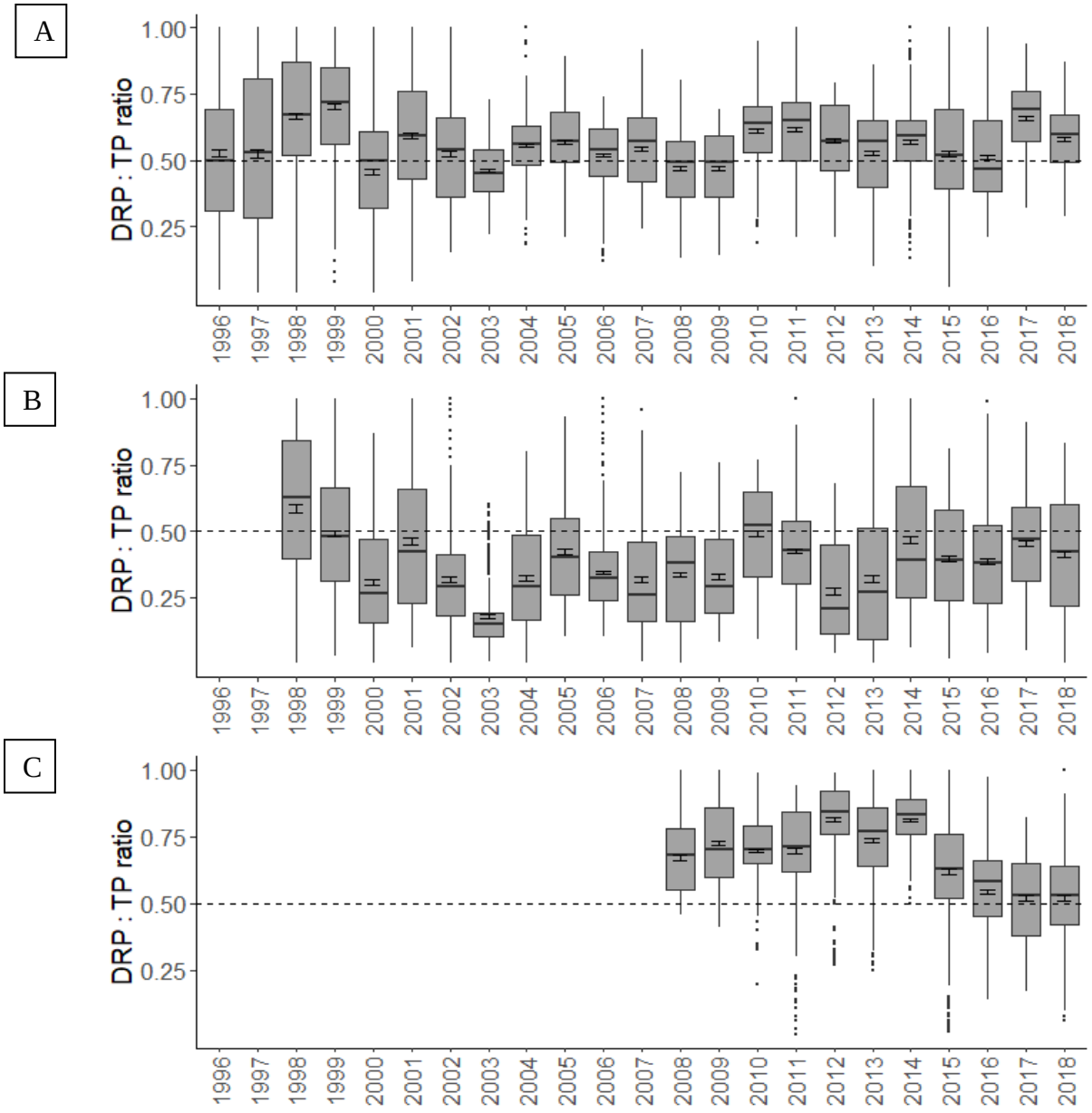

Figure 3.2. Daily DRP:TP ratios at A) Embarras River (EMC), B) Lake Fork - Kaskaskia River (LFK), and C) Salt Fork River (SF). Data under baseflow conditions (<1 mm day^{-1}) were excluded.

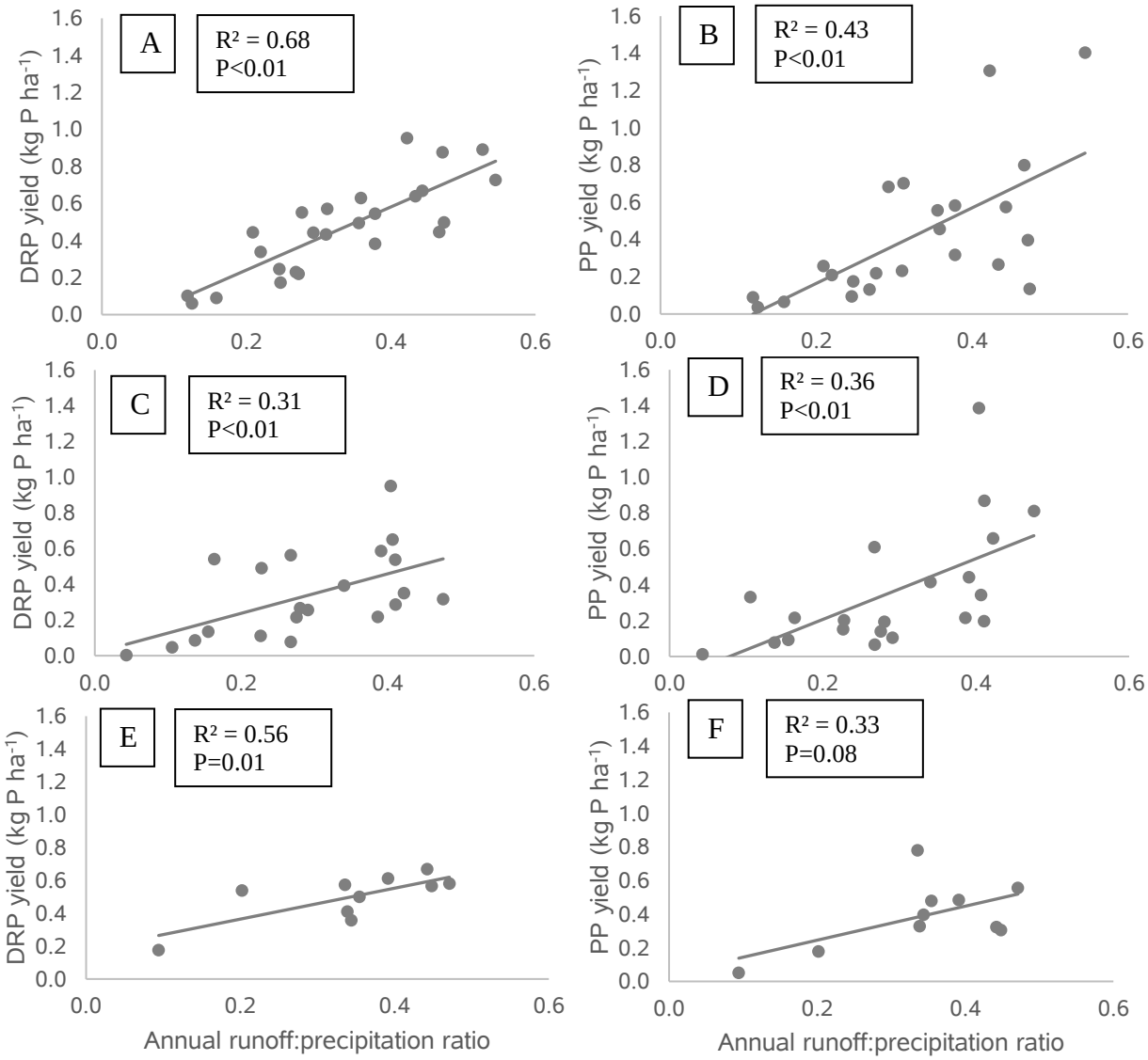

Figure 3.3. Relationship between annual dissolved reactive P (DRP) and particulate P (PP) yields with annual discharge:precipitation ratio at A & B) Embarras River (EMC), C & D) Lake Fork – Kaskaskia River (LFK), and E & F) Salt Fork River (SF) watershed.

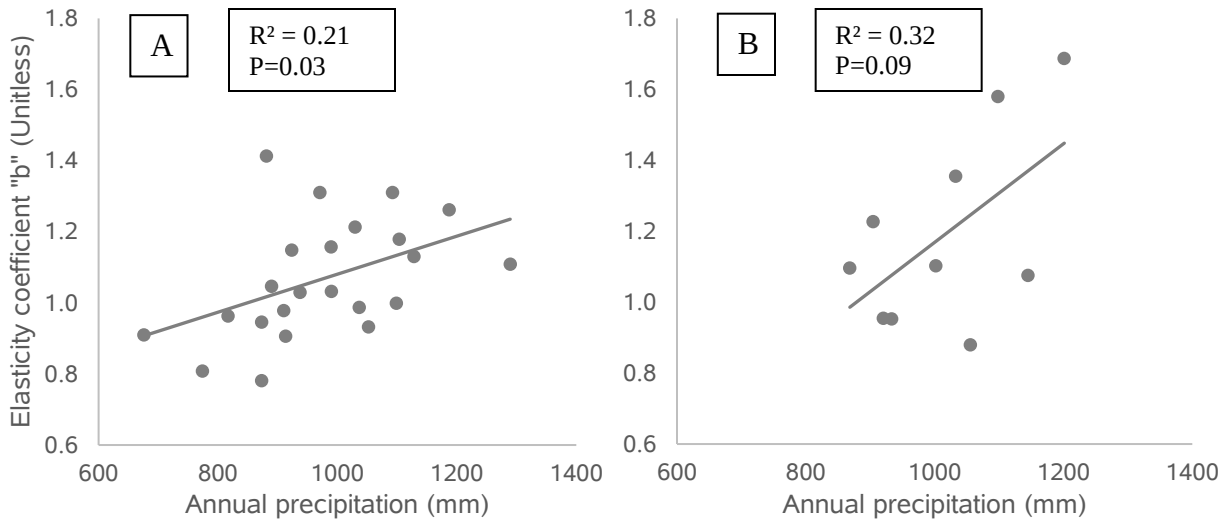

Figure 3.4. Relationship between elasticity coefficient “b” for PP yield and annual precipitation at Embarras River (EMC; P=0.03) and Salt Fork watershed (SF; P=0.09).

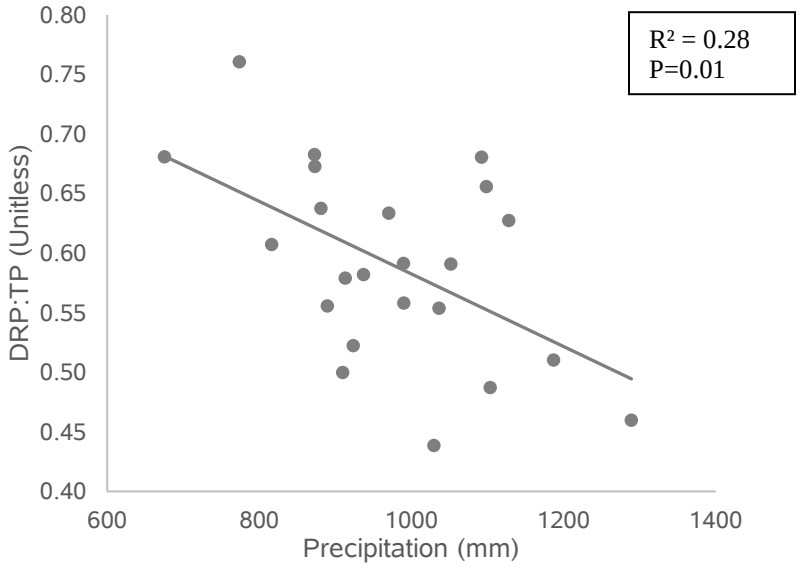

Figure 3.5. Relationship between DRP:TP ratio at daily average runoff >1mm and annual precipitation at Embarras River watershed (EMC).

CHAPTER 4: CONCLUSIONS

The spatial and temporal complexity of processes driving phosphorus (P) dynamics in agricultural systems provides challenges to achieve water quality goals. Expected changes in climatic patterns and rainfall amount, distribution and intensity can exacerbate the detriment of aquatic ecosystems derived from non-point sources. Equally important, there is a need to efficiently produce agricultural goods using finite resources, such as P, that require more information to achieve sustainability. This thesis contributes to improve and communicate our understanding of P loss drivers in agricultural landscapes dominated by artificial subsurface drainage at field and watershed scales. Access to a combination of fine-scale information (sub-meter digital elevation models, individual monitoring of adjacent tile laterals, detailed soil sampling) and long-term datasets allowed the production of robust results in both studies.

The importance of sub-field variability of tile dissolved reactive P (DRP) losses and soil P was highlighted in this study; even relatively small areas can experience substantial changes. These changes can also occur due to topographic characteristics. Closed topographic depressions play an important role in flat agricultural landscapes by being the intersection of water and P-laden soil. Water stored in closed depressions can also solubilize P fertilizer that can be subsequently leached. Based on these findings, it is recommended to target low-lying positions of the field and implement variable rate application. Additionally, it was found that legacy P can contribute to increased tile DRP losses that persist over decades. It was also observed variability across watersheds in the response of P exports to hydrological stimulus. Part of this variability can be explained by differences in the water retention capacity, the influence of baseflow, or external inputs (e.g., sewage treatment plants). Even homogeneously manage fields and watersheds with apparent similarities can experience different responses to P loss drivers.

REFERENCES

Alexander, R. B., Smith, R. A., Schwarz, G. E., Boyer, E. W., Nolan, J. V., and Brakebill, J. W. (2007). Differences in phosphorus and nitrogen delivery to the Gulf of Mexico from the Mississippi River Basin. Environmental science & technology 42, 822-830.

Algoazany, A. S., Kalita, P. K., Czapar, G. F., and Mitchell, J. K. (2007). Phosphorus transport through subsurface drainage and surface runoff from a flat watershed in east central Illinois, USA. Journal of Environmental Quality 36, 681-93.

Amoah, J. K. O., Amatya, D. M., and Nnaji, S. (2012). Quantifying watershed surface depression storage: determination and application in a hydrologic model. Hydrological Processes 27, 2401-2413.

Baffaut, C., Dabney, S. M., Smolen, M. D., Youssef, M. A., Bonta, J. V., Chu, M. L., Guzman, J. A., Shedekar, V., Jha, M. K., and Arnold, J. G. (2015). Hydrologic and water quality modeling: Spatial and temporal considerations. Transactions of the ASABE 58, 1661-1680.

Barton, K. (2016). Multi-model inference. R package version 1.15. 6.; 2016.

Bierman, V. J., Hinz, S. C., Zhu, D.-W., Wiseman, W. J., Rabalais, N. N., and Turner, R. E. (1994). A preliminary mass balance model of primary productivity and dissolved oxygen in the Mississippi River plume/inner Gulf Shelf region. Estuaries 17, 886-899.

Blann, K. L., Anderson, J. L., Sands, G. R., and Vondracek, B. (2009). Effects of agricultural drainage on aquatic ecosystems: a review. Critical Reviews in Environmental Science and Technology 39, 909-1001.

Breitburg, D., Levin, L. A., Oschlies, A., Grégoire, M., Chavez, F. P., Conley, D. J., Garçon, V., Gilbert, D., Gutiérrez, D., Isensee, K., Jacinto, G. S., Limburg, K. E., Montes, I., Naqvi, S. W. A., Pitcher, G. C., Rabalais, N. N., Roman, M. R., Rose, K. A., Seibel, B. A., Telszewski, M., Yasuhara, M., and Zhang, J. (2018). Declining oxygen in the global ocean and coastal waters. Science 359.

Burnham, K. P., and Anderson, D. R. (1998). Practical Use of the Information-Theoretic Approach. In "Model Selection and Inference: A Practical Information-Theoretic Approach", pp. 75-117. Springer New York, New York, NY.

Carpenter, S. R., Caraco, N. F., Correll, D. L., Howarth, R. W., Sharpley, A. N., and Smith, V. H. (1998). Nonpoint pollution of surface waters with phosphorus and nitrogen. Ecological Applications 8, 559-568.

Cermak, J. D., Gilley, J. E., Eghball, B., and Wienhold, B. J. (2004). Leaching and sorption of nitrogen and phosphorus by crop residue. Transactions of the Asae 47, 113-118.

Christianson, L. E., Harmel, R. D., Smith, D., Williams, M. R., and King, K. (2016). Assessment and synthesis of 50 years of published drainage phosphorus losses. Journal of Environmental Quality 45, 1467-1477.

Chun, J. A., and Cooke, R. (2008). Calibrating Agridrain water level control structures using generalized weir and orifice equations. Applied Engineering in Agriculture 24, 595-602.

Clement, D. R., and Steinman, A. D. (2017). Phosphorus loading and ecological impacts from agricultural tile drains in a west Michigan watershed. Journal of Great Lakes Research 43, 50-58.

Cullum, R. F. (2009). Macropore flow estimations under no-till and till systems. Catena 78, 87-91.

David, M. B., Gentry, L. E., and Mitchell, C. A. (2016). Riverine response of sulfate to declining atmospheric sulfur deposition in agricultural watersheds. Journal of environmental quality 45, 1313-1319.
Davis, C. A., Ward, A. S., Burgin, A. J., Loecke, T. D., Riveros-Iregui, D. A., Schnoebelen, D. J., Just, C. L., Thomas, S. A., Weber, L. J., and St. Clair, M. A. (2014). Antecedent Moisture Controls on Stream Nitrate Flux in an Agricultural Watershed. Journal of Environmental Quality 43, 1494-1503.
Diaz, R. J., and Rosenberg, R. (2008). Spreading Dead Zones and Consequences for Marine Ecosystems. Science 321, 926-929.
Djodjic, F., Bergström, L., and Ulén, B. (2002). Phosphorus losses from a structured clay soil in relation to tillage practices. Soil use and Management 18, 79-83.
Dodds, W. K. (2006). Nutrients and the "dead zone": the link between nutrient ratios and dissolved oxygen. in the northern Gulf of Mexico. Frontiers in Ecology and the Environment 4, 211-217.
Doody, D. G., Withers, P. J. A., Dils, R. M., McDowell, R. W., Smith, V., McElarney, Y. R., Dunbar, M., and Daly, D. (2016). Optimizing land use for the delivery of catchment ecosystem services. Frontiers in Ecology and the Environment 14, 325-332.
Duncan, E. W., King, K. W., Williams, M. R., LaBarge, G., Pease, L. A., Smith, D. R., and Fausey, N. R. (2017). Linking soil phosphorus to dissolved phosphorus losses in the Midwest. Agricultural & Environmental Letters 2.
Eastman, M., Gollamudi, A., Stampfli, N., Madramootoo, C. A., and Sarangi, A. (2010). Comparative evaluation of phosphorus losses from subsurface and naturally drained agricultural fields in the Pike River watershed of Quebec, Canada. Agricultural Water Management 97, 596-604.
Fausey, N. R., Brown, L. C., Belcher, H. W., and Kanwar, R. S. (1995). Drainage and Water Quality in Great Lakes and Cornbelt States. Journal of Irrigation and Drainage Engineering 121, 283-288.
Fernández, F. G., and Hoeft, R. G. (2009). Managing soil pH and crop nutrients. Illinois agronomy handbook, 91-112.
Feyereisen, G. W., Francesconi, W., Smith, D. R., Papiernik, S. K., Krueger, E. S., and Wente, C. D. (2015). Effect of replacing surface inlets with blind or gravel inlets on sediment and phosphorus subsurface drainage losses. Journal of Environmental Quality 44, 594-604.
Force, M. R. G. o. M. W. N. T. (2008). Action plan for reducing, mitigating, and controlling hypoxia in the Northern Gulf of Mexico. Office of Wetlands, Oceans, and Watersheds, U.S. Environmental Protection Agency: Washington, DC.
Force, O. L. E. P. T. (2010). Ohio Lake Erie Phosphorus Task Force final report. Retrieved from http://www.epa.state.oh.us/portals/35/lakeerie/ptaskforce/Task_Force_Final_Report_April_2010.pdf.
Fraterrigo, J. M., and Downing, J. A. (2008). The influence of land use on lake nutrients varies with watershed transport capacity. Ecosystems 11, 1021-1034.
Gburek, W. J., Drungil, C. C., Srinivasan, M. S., Needelman, B. A., and Woodward, D. E. (2002). Variable-source-area controls on phosphorus transport: Bridging the gap between research and design. Journal of Soil and Water Conservation 57, 534-543.
Gelbrecht, J., Lengsfeld, H., Pothig, R., and Opitz, D. (2005). Temporal and spatial variation of phosphorus input, retention an loss in a small catchment of NE Germany. Journal of Hydrology 304, 151-165.

Gentry, L. E., David, M. B., Royer, T. V., Mitchell, C. A., and Starks, K. M. (2007). Phosphorus transport pathways to streams in tile-drained agricultural watersheds. Journal of Environmental Quality 36, 408-15.

Ginting, D., Moncrief, J. F., and Gupta, S. C. (2000). Runoff, solids, and contaminant losses into surface tile inlets draining lacustrine depressions. Journal of Environmental Quality 29, 551-560.

Goyette, J.-O., Bennett, E. M., and Maranger, R. (2018a). Differential influence of landscape features and climate on nitrogen and phosphorus transport throughout the watershed. Biogeochemistry.

Goyette, J. O., Bennett, E. M., and Maranger, R. (2018b). Low buffering capacity and slow recovery of anthropogenic phosphorus pollution in watersheds. Nature Geoscience 11, 921-925.

Gu, S., Gruau, G., Dupas, R., Rumpel, C., Crème, A., Fovet, O., Gascuel-Odoux, C., Jeanneau, L., Humbert, G., and Petitjean, P. (2017). Release of dissolved phosphorus from riparian wetlands: Evidence for complex interactions among hydroclimate variability, topography and soil properties. Science of The Total Environment 598, 421-431.

Gu, S., Gruau, G., Malique, F., Dupas, R., Petitjean, P., and Gascuel-Odoux, C. (2018). Drying/rewetting cycles stimulate release of colloidal-bound phosphorus in riparian soils. Geoderma 321, 32-41.

Hayashi, M., van der Kamp, G., and Schmidt, R. (2003). Focused infiltration of snowmelt water in partially frozen soil under small depressions. Journal of Hydrology 270, 214-229.

Heathwaite, L., Haygarth, P., Matthews, R., Preedy, N., and Butler, P. (2005). Evaluating Colloidal Phosphorus Delivery to Surface Waters from Diffuse Agricultural Sources. Journal of Environmental Quality 34, 287-298.

Henderson, R., Kabengi, N., Mantripragada, N., Cabrera, M., Hassan, S., and Thompson, A. (2012). Anoxia-Induced Release of Colloid- and Nanoparticle-Bound Phosphorus in Grassland Soils. Environmental Science & Technology 46, 11727-11734.

Hirsch, R. M., Moyer, D. L., and Archfield, S. A. (2010). Weighted Regressions on Time, Discharge, and Season (WRTDS), with an application to Chesapeake Bay River inputs. JAWRA Journal of the American Water Resources Association 46, 857-880.

Howarth, R. W., and Marino, R. (2006). Nitrogen as the limiting nutrient for eutrophication in coastal marine ecosystems: Evolving views over three decades. Limnology and Oceanography 51, 364-376.

ISGS, and IDOT (2012). Illinois State Geological Survey, and Illinois Department of Transportation,Illinois Height Modernization Program, 2002-2013, Illinois LiDAR county database: Illinois State Geological Survey, http://www.isgs.uiuc.edu/nsdihome/webdocs/ilhmp/data.html (accessed Mar 29, 2016).

Jacobson, L. M., David, M. B., and Drinkwater, L. E. (2011). A spatial analysis of phosphorus in the Mississippi River Basin. Journal of Environmental Quality 40, 931-941.

Jarvie, H. P., Sharpley, A. N., Spears, B., Buda, A. R., May, L., and Kleinman, P. J. A. (2013). Water Quality Remediation Faces Unprecedented Challenges from "Legacy Phosphorus". Environmental Science & Technology 47, 8997-8998.

Jarvis, N. J. (2007). A review of non-equilibrium water flow and solute transport in soil macropores: principles, controlling factors and consequences for water quality. European Journal of Soil Science 58, 523-546.

Jaynes, D. B., Colvin, T. S., and Kaspar, T. C. (2005). Identifying potential soybean management zones from multi-year yield data. Computers and Electronics in Agriculture 46, 309-327.
Jaynes, D. B., Kaspar, T., Colvin, T., and James, D. (2003). Cluster Analysis of Spatiotemporal Corn Yield Patterns in an Iowa Field. Agronomy Journal - AGRON J 95.
Kalita, P. K., Algoazany, A. S., Mitchell, J. K., Cooke, R. A. C., and Hirschi, M. C. (2006). Subsurface water quality from a flat tile-drained watershed in Illinois, USA. Agriculture Ecosystems & Environment 115, 183-193.
King, K., Williams, M., and Fausey, N. (2016). Effect of crop type and season on nutrient leaching to tile drainage under a corn–soybean rotation. Journal of soil and water conservation 71, 56-68.
King, K. W., Williams, M. R., and Fausey, N. R. (2015a). Contributions of systematic tile drainage to watershed-scale phosphorus transport. Journal of Environmental Quality 44, 486-94.
King, K. W., Williams, M. R., LaBarge, G. A., Smith, D. R., Reutter, J. M., Duncan, E. W., and Pease, L. A. (2018). Addressing agricultural phosphorus loss in artificially drained landscapes with 4R nutrient management practices. Journal of Soil and Water Conservation 73, 35-47.
King, K. W., Williams, M. R., Macrae, M. L., Fausey, N. R., Frankenberger, J., Smith, D. R., Kleinman, P. J. A., and Brown, L. C. (2015b). Phosphorus transport in agricultural subsurface drainage: a review. Journal of Environmental Quality 44, 467-485.
Kleinman, P. J. A., Sharpley, A. N., McDowell, R. W., Flaten, D. N., Buda, A. R., Tao, L., Bergstrom, L., and Zhu, Q. (2011). Managing agricultural phosphorus for water quality protection: principles for progress. Plant and Soil 349, 169-182.
Letkeman, L. P., Tiessen, H., and Campbell, C. A. (1996). Phosphorus transformations and redistribution during pedogenesis of western Canadian soils. Geoderma 71, 201-218.
Macrae, M. L., English, M. C., Schiff, S. L., and Stone, M. (2007). Intra-annual variability in the contribution of tile drains to basin discharge and phosphorus export in a first-order agricultural catchment. Agricultural Water Management 92, 171-182.
McDowell, R. W., and Sharpley, A. N. (2001). Approximating phosphorus release from soils to surface runoff and subsurface drainage. Journal of Environmental Quality 30, 508-520.
McDowell, R. W., and Sharpley, A. N. (2002). The effect of antecedent moisture conditions on sediment and phosphorus loss during overland flow: Mahantango Creek catchment, Pennsylvania, USA. Hydrological Processes 16, 3037-3050.
McMillan, S. K., Wilson, H. F., Tague, C. L., Hanes, D. M., Inamdar, S., Karwan, D. L., Loecke, T., Morrison, J., Murphy, S. F., and Vidon, P. (2018). Before the storm: antecedent conditions as regulators of hydrologic and biogeochemical response to extreme climate events. Biogeochemistry.
Mekonnen, M. M., and Hoekstra, A. Y. (2018). Global Anthropogenic Phosphorus Loads to Freshwater and Associated Grey Water Footprints and Water Pollution Levels: A High-Resolution Global Study. Water Resources Research, n/a-n/a.
Messiga, A. J., Ziadi, N., Morel, C., and Parent, L. E. (2010). Soil phosphorus availability in no-till versus conventional tillage following freezing and thawing cycles. Canadian Journal of Soil Science 90, 419-428.
Michalak, A. M., Anderson, E. J., Beletsky, D., Boland, S., Bosch, N. S., Bridgeman, T. B., Chaffin, J. D., Cho, K., Confesor, R., and Daloğlu, I. (2013). Record-setting algal bloom

in Lake Erie caused by agricultural and meteorological trends consistent with expected future conditions. Proceedings of the National Academy of Sciences 110, 6448-6452.
Muggeo, V. M. (2008). Segmented: an R package to fit regression models with broken-line relationships. R news 8, 20-25.
Mulla, D. J., Sekely, A. C., and Beatty, M. (2000). Evaluation of remote sensing and targeted soil sampling for variable rate application of lime. Proceedings of the 5th International Conference on Precision Agriculture, Bloomington, Minnesota, USA, 16-19 July, 2000, 1-14.
Murphy, J. C., Hirsch, R. M., and Sprague, L. A. (2014). Antecedent flow conditions and nitrate concentrations in the Mississippi River basin. Hydrol. Earth Syst. Sci. 18, 967-979.
Nash, P. R., Nelson, K. A., Motavalli, P. P., Nathan, M., and Dudenhoeffer, C. (2014). Reducing phosphorus loss in tile water with managed drainage in a claypan soil. Journal of Environmental Quality 44, 585-593.
NOAA (2017). National Centers for Environmental Information. Historical daily conditions . Available online at https://gis.ncdc.noaa.gov/maps/ncei. Accessed [July/25/2018].
Page, T., Haygarth, P. M., Beven, K. J., Joynes, A., Butler, T., Keeler, C., Freer, J., Owens, P. N., and Wood, G. A. (2005). Spatial variability of soil phosphorus in relation to the topographic index and critical source areas. Journal of Environmental Quality 34, 2263-2277.
Pease, L. A., King, K. W., Williams, M. R., LaBarge, G. A., Duncan, E. W., and Fausey, N. R. (2018). Phosphorus export from artificially drained fields across the Eastern Corn Belt. Journal of Great Lakes Research.
Pinhero, J., Bates, D., Debroy, S., and Sarkar, D. (2017). R Core Team (2017) nlme: linear and nonlinear mixed effects models. R package version 3.1-131.
Pionke, H. B., Gburek, W. J., and Sharpley, A. N. (2000). Critical source area controls on water quality in an agricultural watershed located in the Chesapeake Basin. Ecological Engineering 14, 325-335.
Planchon, O., and Darboux, F. (2002). A fast, simple and versatile algorithm to fill the depressions of digital elevation models. Catena 46, 159-176.
Poirier, S. C., Whalen, J. K., and Michaud, A. R. (2012). Bioavailable phosphorus in fine-sized sediments transported from agricultural fields. Soil Science Society of America Journal 76, 258-267.
Quinton, J. N., Govers, G., Van Oost, K., and Bardgett, R. D. (2010). The impact of agricultural soil erosion on biogeochemical cycling. Nature Geoscience 3, 311.
Roth, J., and Capel, P. (2012). The hydrology of a drained topographical depression within an agricultural field in north-central Iowa. Transactions of the ASABE 55, 1801-1814.
Rowe, H., Withers, P. J. A., Baas, P., Chan, N. I., Doody, D., Holiman, J., Jacobs, B., Li, H., MacDonald, G. K., McDowell, R., Sharpley, A. N., Shen, J., Taheri, W., Wallenstein, M., and Weintraub, M. N. (2016). Integrating legacy soil phosphorus into sustainable nutrient management strategies for future food, bioenergy and water security. Nutrient Cycling in Agroecosystems 104, 393-412.
Royer, T. V., David, M. B., and Gentry, L. E. (2006). Timing of riverine export of nitrate and phosphorus from agricultural watersheds in Illinois: Implications for reducing nutrient loading to the Mississippi River. Environmental Science & Technology 40, 4126-4131.

Sallade, Y. E., and Sims, J. T. (1997). Phosphorus Transformations in the Sediments of Delaware's Agricultural Drainageways: II. Effect of Reducing Conditions on Phosphorus Release. Journal of Environmental Quality 26, 1579-1588.
Schilling, K. E., Kim, S. W., Jones, C. S., and Wolter, C. F. (2017). Orthophosphorus contributions to total phosphorus concentrations and loads in Iowa agricultural watersheds. J Environ Qual 46, 828-835.
Schindler, D. W., Hecky, R., Findlay, D., Stainton, M., Parker, B., Paterson, M., Beaty, K., Lyng, M., and Kasian, S. (2008). Eutrophication of lakes cannot be controlled by reducing nitrogen input: results of a 37-year whole-ecosystem experiment. Proceedings of the National Academy of Sciences 105, 11254-11258.
Sharpley, A., Jarvie, H. P., Buda, A., May, L., Spears, B., and Kleinman, P. (2013). Phosphorus legacy: overcoming the effects of past management practices to mitigate future water quality impairment. Journal of Environmental Quality 42, 1308-1326.
Sharpley, A. N., Chapra, S. C., Wedepohl, R., Sims, J. T., Daniel, T. C., and Reddy, K. R. (1994). Managing Agricultural Phosphorus for Protection of Surface Waters: Issues and Options. Journal of Environmental Quality 23, 437-451.
Sharpley, A. N., Weld, J. L., Beegle, D. B., Kleinman, P. J. A., Gburek, W. J., Moore, P. A., and Mullins, G. (2003). Development of phosphorus indices for nutrient management planning strategies in the United States. Journal of Soil and Water Conservation 58, 137-152.
Shober, A. L., and Sims, J. T. (2009). Evaluating Phosphorus Release from Biosolids and Manure-Amended Soils under Anoxic Conditions. Journal of Environmental Quality 38, 309-318.
Sims, J. T., Simard, R. R., and Joern, B. C. (1998). Phosphorus loss in agricultural drainage: Historical perspective and current research. Journal of Environmental Quality 27, 277-293.
Smith, D., Livingston, S., Zuercher, B., Larose, M., Heathman, G., and Huang, C. (2008). Nutrient losses from row crop agriculture in Indiana. Journal of Soil and Water Conservation 63, 396-409.
Smith, D. R., King, K. W., Johnson, L., Francesconi, W., Richards, P., Baker, D., and Sharpley, A. N. (2015a). Surface runoff and tile drainage transport of phosphorus in the midwestern United States. Journal of Environmental Quality 44, 495-502.
Smith, D. R., King, K. W., and Williams, M. R. (2015b). What is causing the harmful algal blooms in Lake Erie? Journal of Soil and Water Conservation 70, 27A-29A.
Smith, D. R., and Livingston, S. J. (2013). Managing farmed closed depressional areas using blind inlets to minimize phosphorus and nitrogen losses. Soil Use and Management 29, 94-102.
Stackpoole, S. M., Stets, E. G., and Sprague, L. A. (2019). Variable impacts of contemporary versus legacy agricultural phosphorus on US river water quality. Proceedings of the National Academy of Sciences 116, 20562-20567.
Sterner, R. W. (2008). On the phosphorus limitation paradigm for lakes. International Review of Hydrobiology 93, 433-445.
Sugg, Z. (2007). Assessing US Farm Drainage: Can GIS Lead to Better Estimates of Subsurface Drainage Extent? World Resources Institute, Washington, DC. .

Suriyavirun, N., Krichels, A. H., Kent, A. D., and Yang, W. H. (2019). Microtopographic differences in soil properties and microbial community composition at the field scale. Soil Biology and Biochemistry 131, 71-80.

Team, R. C. D. (2017). R: a language and environment for statistical computing. R Foundation for Statistical Computing, Vienna, Austria. ISBN3-900051-07-0 https://www. R-project. org.

Thoma, D. P., Gupta, S. C., Strock, J. S., and Moncrief, J. F. (2005). Tillage and nutrient source effects on water quality and corn grain yield from a flat landscape. Journal of Environmental Quality 34, 1102-1111.

Thomas, I. A., Mellandera, P. E., Murphy, P. N. C., Fenton, O., Shine, O., Djodjic, F., Dunlop, P., and Jordan, P. (2016). A sub-field scale critical source area index for legacy phosphorus management using high resolution data. Agriculture Ecosystems & Environment 233, 238-252.

Tomer, M. D., and Liebman, M. (2014). Nutrients in soil water under three rotational cropping systems, Iowa, USA. Agriculture Ecosystems & Environment 186, 105-114.

Tomer, M. D., Wilson, C. G., Moorman, T. B., Cole, K. J., Heer, D., and Isenhart, T. M. (2010). Source-Pathway Separation of Multiple Contaminants during a Rainfall-Runoff Event in an Artificially Drained Agricultural Watershed All rights reserved. No part of this periodical may be reproduced or transmitted in any form or by any means, electronic or mechanical, including photocopying, recording, or any information storage and retrieval system, without permission in writing from the publisher. Journal of Environmental Quality 39, 882-895.

Turner, R. E., and Rabalais, N. N. (2003). Linking landscape and water quality in the Mississippi river basin for 200 years. Bioscience 53, 563-572.

Ulén, B., Aronsson, H., Bechmann, M., Krogstad, T., Øygarden, L., and Stenberg, M. (2010). Soil tillage methods to control phosphorus loss and potential side-effects: a Scandinavian review. Soil Use and Management 26, 94-107.

USDA-NRCS, S. S. S. (2016). Gridded Soil Survey Geographic (gSSURGO) Database for Douglas County, Illinois. Available online at https://gdg.sc.egov.usda.gov/. Accessed [September/02/2016].

Van Esbroeck, C. J., Macrae, M. L., Brunke, R. I., and McKague, K. (2016). Annual and seasonal phosphorus export in surface runoff and tile drainage from agricultural fields with cold temperate climates. Journal of Great Lakes Research 42, 1271-1280.

Van Esbroeck, C. J., Macrae, M. L., Brunke, R. R., and McKague, K. (2017). Surface and subsurface phosphorus export from agricultural fields during peak flow events over the nongrowing season in regions with cool, temperate climates. Journal of Soil and Water Conservation 72, 65-76.

Vidon, P., and Cuadra, P. E. (2010). Impact of precipitation characteristics on soil hydrology in tile-drained landscapes. Hydrological Processes 24, 1821-1833.

Vidon, P., Hubbard, L. E., and Soyeux, E. (2009). Seasonal solute dynamics across land uses during storms in glaciated landscape of the US Midwest. Journal of Hydrology 376, 34-47.

White, M. J., Storm, D. E., Busteed, P. R., Stoodley, S. H., and Phillips, S. J. (2009). Evaluating nonpoint source critical source area contributions at the watershed scale. Journal of Environmental Quality 38, 1654-1663.

Williams, M. R., King, K. W., Duncan, E. W., Pease, L. A., and Penn, C. J. (2018). Fertilizer placement and tillage effects on phosphorus concentration in leachate from fine-textured soils. Soil and Tillage Research 178, 130-138.

Williams, M. R., King, K. W., Ford, W., Buda, A. R., and Kennedy, C. D. (2016). Effect of tillage on macropore flow and phosphorus transport to tile drains. Water Resources Research 52, 2868-2882.

Williams, M. R., Livingston, S. J., Heathman, G. C., and McAfee, S. J. (2019). Thresholds for run-off generation in a drained closed depression. Hydrological Processes 33, 2408-2421.

Wilson, H. F., Satchithanantham, S., Moulin, A. P., and Glenn, A. J. (2016). Soil phosphorus spatial variability due to landform, tillage, and input management: A case study of small watersheds in southwestern Manitoba. Geoderma 280, 14-21.

Xue, Y., David, M. B., Gentry, L. E., and Kovacic, D. A. (1998). Kinetics and modeling of dissolved phosphorus export from a tile-drained agricultural watershed. Journal of Environmental Quality 27, 917-922.

Young, E. O., and Ross, D. S. (2001). Phosphate Release from Seasonally Flooded Soils. Journal of Environmental Quality 30, 91-101.

Zhang, Q., and Ball, W. P. (2017). Improving riverine constituent concentration and flux estimation by accounting for antecedent discharge conditions. Journal of Hydrology 547, 387-402.

APPENDIX A: SUPPLEMENTARY MATERIAL FOR CHAPTER 2

Table A1. Contributing area, depression index, soil test P (STP) concentration and management practices of 36 instrumented tiles.

Tile	Area drained (ha)	Depression index (m ha^{-1})	Crop rotation[1] HY:2015/2016/2017	Mean Bray P-1 soil test (mg kg^{-1}) and STD[2]	P fertilizer source
1	1.91	2425	C / S / C	26.14 (11.52)	Unfertilized
2	1.84	1161	C / S / C	21.63 (8.56)	Unfertilized
3	1.82	518	C / S / C	23.06 (4.04)	Unfertilized
4	1.80	167	C / S / C	25.12 (7.67)	Unfertilized
5	1.78	118	C / S / C	19.04 (5.10)	Unfertilized
6	1.72	193	C / S / C	22.97 (5.52)	Unfertilized
7	1.65	425	C / S / C	20.47 (7.73)	Unfertilized
8	1.59	321	C / S / C	20.74 (5.61)	Unfertilized
9	1.52	125	C / S / C	23.24 (4.30)	Unfertilized
10	1.45	61	C / S / C	22.01 (6.85)	Unfertilized
11	1.38	51	C / S / C	19.11 (7.08)	Unfertilized
12	1.30	40	C / S / C	17.43 (5.42)	Unfertilized
13	1.53	898	C / S / C	31.82 (18.47)	Unfertilized
14	1.60	1000	C / S / C	20.65 (9.77)	Unfertilized
15	1.66	679	C / S / C	25.56 (11.43)	Unfertilized
16	1.70	1606	C / S / C	39.42 (10.03)	Unfertilized
17	1.69	351	C / S / C	23.06 (8.29)	Unfertilized
18	1.59	258	C / S / C	28.07 (10.46)	Unfertilized
19	1.59	714	S / C / S	43.80 (4.14)	DAP
20	1.66	869	S / C / S	32.18 (14.48)	TSP
21	1.67	515	S / C / S	26.01 (8.47)	DAP
22	1.68	472	S / C / S	14.12 (2.31)	DAP
23	1.71	487	S / C / S	25.21 (7.76)	TSP
24	1.71	652	S / C / S	24.76 (9.12)	DAP
25	1.74	457	S / C / S	46.57 (15.60)	DAP
26	1.75	156	S / C / S	44.96 (14.65)	DAP
27	1.77	159	S / C / S	38.70 (13.00)	DAP
28	1.79	359	S / C / S	35.75 (17.06)	TSP
29	1.81	477	S / C / S	33.07 (9.87)	DAP
30	1.47	239	S / C / S	34.86 (7.13)	DAP
31	1.60	119	S / C / S	27.98 (11.02)	DAP
32	1.58	72	S / C / S	27.17 (12.30)	TSP
33	1.58	382	S / C / S	32.54 (11.12)	DAP
34	1.58	275	S / C / S	41.47 (23.38)	DAP
35	1.58	134	S / C / S	46.48 (26.04)	DAP
36	1.58	144	S / C / S	48.80 (45.86)	TSP

[1] Crop rotation: C=corn; S=soybean.
[2]STD: Standard deviation of the mean.

Table A2. Annual yield and flow-weighted mean concentration (FWMC) of DRP in 36 tiles from 2015 to 2017.

Tile	FWMC of DRP (mg L^{-1})			DRP yield (kg ha^{-1})		
	2015	2016	2017	2015	2016	2017
1	0.078	0.054	0.055	0.148	0.160	0.178
2	0.018	0.008	0.015	0.037	0.026	0.049
3	0.015	0.008	0.015	0.029	0.021	0.040
4	0.010	0.010	0.017	0.021	0.028	0.056
5	0.014	0.010	0.015	0.029	0.027	0.035
6	0.008	0.008	0.012	0.018	0.026	0.041
7	0.014	0.010	0.044	0.030	0.033	0.128
8	0.011	0.011	0.026	0.025	0.033	0.077
9	0.007	0.009	0.020	0.017	0.030	0.061
10	0.008	0.008	0.014	0.019	0.027	0.047
11	0.008	0.010	0.013	0.018	0.033	0.045
12	0.007	0.010	0.012	0.014	0.026	0.036
13	0.029	0.016	0.028	0.058	0.052	0.088
14	0.018	0.015	0.022	0.038	0.048	0.070
15	0.010	0.014	0.018	0.021	0.046	0.052
16	0.049	0.027	0.049	0.106	0.079	0.154
17	0.021	0.021	0.020	0.042	0.065	0.061
18	0.018	0.015	0.025	0.039	0.043	0.070
19	0.025	0.062	0.061	0.023	0.100	0.115
20	0.029	0.029	0.030	0.054	0.058	0.082
21	0.036	0.048	0.047	0.053	0.106	0.113
22	0.010	0.015	0.019	0.018	0.035	0.051
23	0.021	0.019	0.028	0.044	0.050	0.090
24	0.040	0.039	0.042	0.079	0.101	0.123
25	0.044	0.041	0.069	0.076	0.114	0.187
26	0.035	0.029	0.038	0.061	0.077	0.104
27	0.009	0.013	0.016	0.019	0.039	0.062
28	0.028	0.024	0.022	0.059	0.077	0.083
29	0.048	0.021	0.024	0.103	0.071	0.083
30	0.030	0.027	0.076	0.062	0.081	0.263
31	0.014	0.020	0.034	0.028	0.052	0.128
32	0.010	0.011	0.029	0.018	0.021	0.087
33	-	0.044	0.047	-	0.127	0.151
34	0.031	0.036	0.049	0.060	0.098	0.159
35	0.022	0.038	0.035	0.043	0.108	0.126
36	0.044	0.051	0.109	0.084	0.123	0.384
Average	0.024	0.023	0.033	0.046	0.062	0.102
Std. deviation	0.016	0.015	0.021	0.031	0.037	0.070

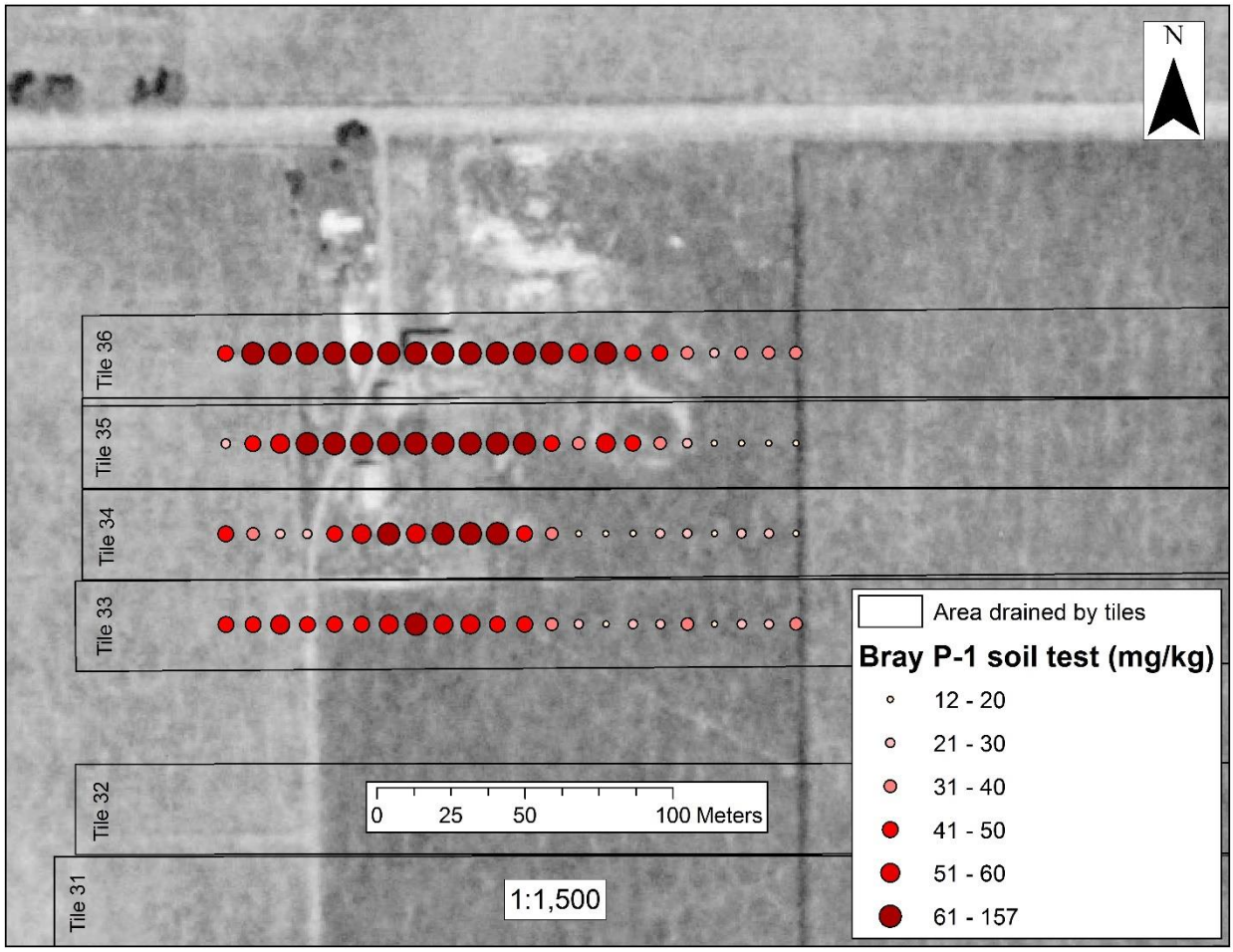

Figure A1. Aerial image from 1940 and soil test P (STP) concentrations of the area with legacy P store from past land management in tiles 33 to 36. Aerial image source: Illinois State Geological Survey, Unpublished material. Image: AO-3A-14. Retrieved from URL: https://clearinghouse.isgs.illinois.edu/data/imagery/1937-1947-illinois-historical-aerial-photography

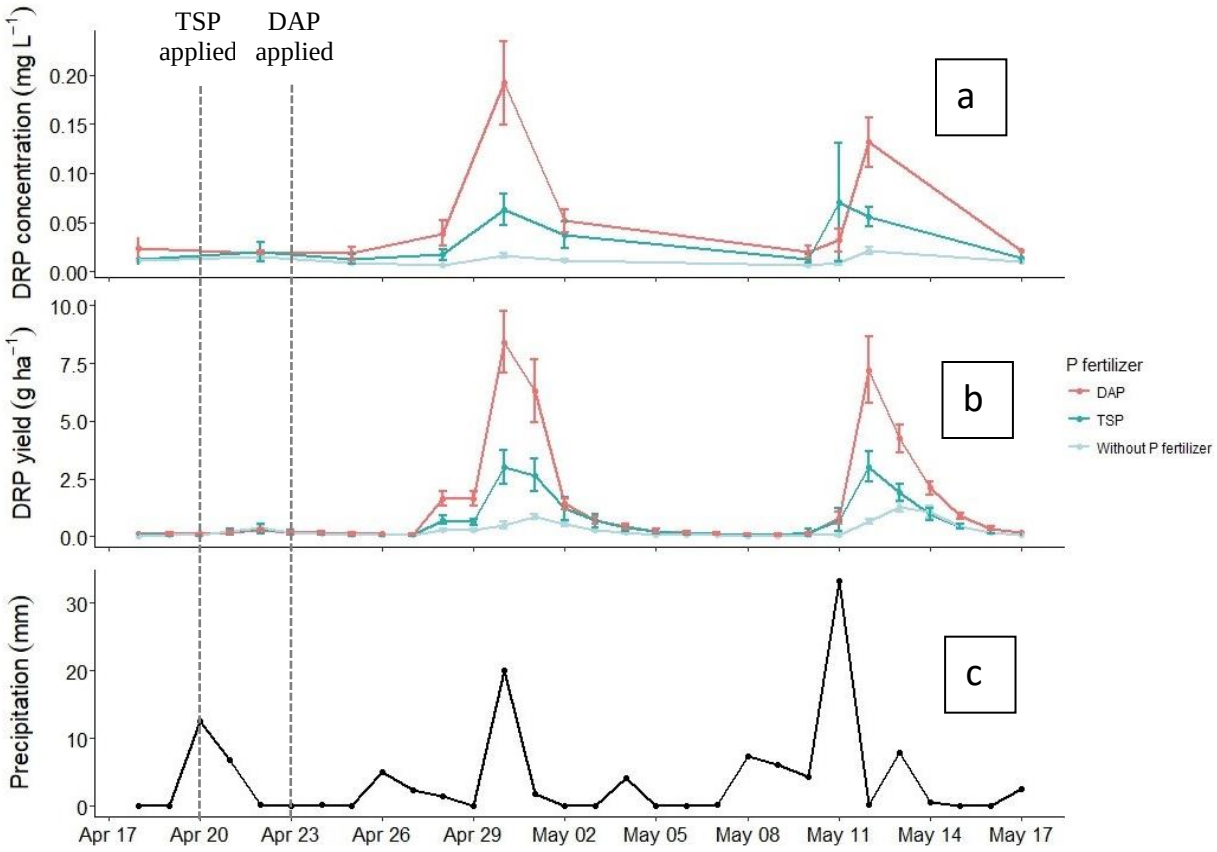

Figure A2. Mean ± 1 SE of a) DRP concentration from discrete water samples, b) interpolated daily DRP yield, and c) daily precipitation in the study site. Triple superphosphate (TSP) was applied on April 20th 2016 and diammonium phosphate (DAP) on April 23rd 2016.

APPENDIX B: SUPPLEMENTARY MATERIAL FOR CHAPTER 3

Appendix B1. Flow anomalies included in the Weighted Regressions on Time, Discharge, and Season mopdel.

Long-term FA (preceding 1-year vs. entire period):

$$LTFA(t) = X_{year}(t) - X_{entire\ period} \quad (4)$$

Mid-term FA (preceding 1-month vs. preceding 1-year):

$$MTFA(t) = X_{month}(t) - X_{year}(t) \quad (5)$$

Short-term FA (current day vs. preceding 1-month):

$$STAF(t) = X_{current\ day}(t) - X_{month}(t) \quad (6)$$

Annual FA (preceding 1-year vs. preceding 5-year):

$$AnnualFA(t) = X_{year}(t) - X_{5year}(t) \quad (7)$$

Seasonal FA (preceding quarter-year vs. preceding 1-year):

$$SeasonFA(t) = X_{0.25year}(t) - X_{year}(t) \quad (8)$$

Daily FA (current day vs. preceding quarter-year):

$$DailyFA(t) = X_{current\ day}(t) - X_{0.25}(t) \quad (9)$$

100-day FA (preceding 100-day vs. entire period):

$$FA100(t) = X_{100day}(t) - X_{entire\ period} \quad (10)$$

10-day FA (preceding 10-day vs. preceding 100-day):

$$FA10(t) = X_{10day}(t) - X_{100\ day}(t) \quad (11)$$

1-day FA (current day vs. preceding 10-day):

$$FAA1(t) = X_{current\ day}(t) - X_{10\ day}(t) \quad (12)$$

Where X is the average of log-transformed daily discharge.

$$ADF(t) = \frac{\sum_{j=1}^{J} d^{t-t_j} Q_{t_j}}{\sum_{j=1}^{J} d^{t-t_j}} \quad (13)$$

Where J is the max. num. of discharge observations, t is the day, t_j is a historical day relative to t

$$dQ/dt(t) = Q_t - Q_{t-1} \quad (14)$$

Where Q is flow, t is the day;

$$BFI(t) = BF_t/Q_t \quad (15)$$

Where BF_t is the baseflow of the day and Q is flow.

$$E = 1 - \frac{\sum_{i=1}^{n} \left| Y_i^{obs} - Y_i^{est} \right|^2}{\sum_{i=1}^{n} \left| Y_i^{obs} - Y_i^{mean} \right|^2} \quad (16)$$

Where E is the modified Nash-Sutcliffe efficiency coefficient.

Table B1. Annual precipitation, discharge, DRP yields and PP yields at Embarras River (EMC), Lake Fork (LFK), and Salt Fork (SF) watersheds located in east-central Illinois.

Hydrol. year	Precipitation			Discharge			DRP yields			PP yields		
	EMC	LFK	SF	EMC	LFK	SF	EMC	LFK	SF	EMC	LFK	SF
	mm			mm			kg P ha^{-1}			kg P ha^{-1}		
1994	925			487			0.891					
1995	955			260			0.221					
1996	817			387			0.498			0.134		
1997	971			284			0.442			0.683		
1998	1092	1128		474	463		0.639	0.537		0.265	0.197	
1999	881	901		273	248		0.433	0.215		0.232	0.140	
2000	676	879		107	120		0.090	0.085		0.066	0.077	
2001	774	889		190	259		0.247	0.256		0.094	0.105	
2002	1104	1149		601	485		0.727	0.350		1.405	0.659	
2003	924	771		109	81		0.101	0.046		0.089	0.332	
2004	990	823		352	338		0.495	0.287		0.557	0.869	
2005	1052	1007		377	394		0.629	0.587		0.456	0.443	
2006	910	916		225	207		0.174	0.110		0.175	0.152	
2007	913	1052		253	240		0.551	0.489		0.218	0.202	
2008	1289	1481		544	598		0.953	0.951		1.307	1.386	
2009	1030	1117	1002	481	531	449	0.446	0.316	0.566	0.800	0.812	0.307
2010	1128	1322	1145	532	538	506	0.877	0.650	0.669	0.397	0.342	0.323
2011	890	855	933	336	330	316	0.382	0.216	0.411	0.317	0.216	0.329
2012	873	735	920	109	32	87	0.061	0.003	0.176	0.036	0.013	0.051
2013	937	1004	868	354	342	409	0.545	0.392	0.581	0.582	0.415	0.557
2014	1036	1096	1056	217	179	213	0.444	0.541	0.538	0.257	0.215	0.179
2015	990	965	1098	266	258	430	0.231	0.077	0.612	0.131	0.066	0.485
2016	1187	1333	1201	370	356	403	0.571	0.562	0.574	0.703	0.610	0.781
2017	873	818	905	387	229	311	0.669	0.265	0.358	0.575	0.193	0.398
2018	1099	1066	1033	242	165	366	0.339	0.135	0.500	0.210	0.092	0.480
Average	973	1015	1016	329	304	349	0.466	0.337	0.498	0.421	0.359	0.389
Std. Dev.	132	191	105	135	152	117	0.244	0.235	0.139	0.362	0.332	0.193

Table B2. Elasticity coefficient "b" for DRP and PP yields at three watersheds in east-central Illinois. Baseflow was defined as area-weighted flow < 1mm day^{-1}.

Hydrol. year	Embarras (EMC)				Lake Fork - Kaskaskia (LFK)				Salf Fork (SF)			
	DRP		PP		DRP		PP		DRP		PP	
	Entire dataset	Non-baseflow fraction	Entire dataset	Non-baseflow fraction	Entire dataset	Non-baseflow fraction	Entire dataset	Non-baseflow fraction	Entire dataset	Non-baseflow fraction	Entire dataset	Non-baseflow fraction
	----------Elasticity coefficient (b)----------											
1994	1.02	1.57										
1995	0.98	1.34										
1996	1.06	1.53	0.96	0.90								
1997	1.02	1.85	1.31	1.68								
1998	1.02	1.83	1.31	1.39	1.15	1.73	0.93	1.39				
1999	1.09	1.90	1.41	1.42	1.03	1.71	1.00	1.24				
2000	1.07	2.08	0.91	NA	1.00	1.53	0.85	1.61				
2001	1.04	1.75	0.81	1.91	0.98	2.08	0.75	1.33				
2002	1.02	1.77	1.18	1.87	0.99	1.91	0.91	1.92				
2003	1.14	1.77	1.15	1.38	1.21	1.87	1.25	1.66				
2004	1.13	1.92	1.16	2.14	1.20	1.80	1.04	1.93				
2005	0.92	1.98	0.93	1.96	0.97	2.16	0.82	2.05				
2006	0.83	2.07	0.98	2.02	0.96	2.12	0.87	2.00				
2007	0.84	2.40	0.91	1.81	1.06	2.25	0.71	1.80				
2008	1.08	2.01	1.11	1.91	1.26	2.01	1.03	1.78				
2009	1.11	1.50	1.21	1.49	1.16	1.54	0.96	1.50	0.68	1.09	1.10	1.20
2010	1.07	1.73	1.13	1.45	1.15	1.73	0.88	1.46	0.93	1.23	1.08	1.15
2011	0.88	1.79	1.05	1.64	0.88	1.94	0.82	1.75	0.62	1.66	0.95	1.91
2012	0.63	2.40	0.78	1.87	0.62	NA	0.71	NA	0.44	1.39	0.95	1.42
2013	1.01	2.04	1.03	2.00	0.99	2.19	0.91	2.01	0.63	1.42	1.10	1.89
2014	0.97	2.28	0.99	1.81	1.06	2.50	0.82	2.19	0.59	1.20	0.88	1.45
2015	0.92	2.31	1.03	1.08	0.58	2.13	0.71	1.39	1.40	1.46	1.58	1.53
2016	0.99	1.95	1.26	1.98	0.84	2.40	0.91	2.14	1.53	1.63	1.69	1.91
2017	0.90	1.71	0.95	1.97	0.79	2.24	0.68	2.22	1.43	1.62	1.23	1.86
2018	1.06	1.78	1.00	1.76	1.03	2.25	0.87	1.99	1.51	1.66	1.35	1.70
Average	0.99	1.89	1.07	1.70	1.00	2.00	0.88	1.77	0.97	1.44	1.19	1.60

Table B3. Average daily DRP:TP ratios at the three watersheds. Baseflow was defined as area-weighted flow < 1mm day^{-1}.

Year	Embarras (EMC)		Lake Fork - Kaskaskia (LFK)		Salt Fork (SF)	
	Entire dataset	Non-baseflow fraction	Entire dataset	Non-baseflow fraction	Entire dataset	Non-baseflow fraction
	---------- DRP:TP----------					
1996	0.53	0.61				
1997	0.53	0.63	0.07			
1998	0.67	0.68	0.58	0.69		
1999	0.70	0.64	0.49	0.58		
2000	0.46	0.68	0.31	0.63		
2001	0.59	0.76	0.46	0.68		
2002	0.52	0.49	0.32	0.39		
2003	0.46	0.52	0.18	0.21		
2004	0.56	0.59	0.32	0.38		
2005	0.57	0.59	0.42	0.56		
2006	0.52	0.50	0.34	0.43		
2007	0.54	0.58	0.32	0.56		
2008	0.47	0.46	0.33	0.40		
2009	0.47	0.44	0.33	0.36	0.72	0.64
2010	0.61	0.63	0.49	0.59	0.70	0.66
2011	0.62	0.56	0.43	0.52	0.70	0.61
2012	0.57	0.67	0.27	0.19	0.82	0.67
2013	0.53	0.58	0.32	0.56	0.74	0.65
2014	0.57	0.55	0.47	0.62	0.81	0.74
2015	0.52	0.56	0.40	0.50	0.62	0.60
2016	0.51	0.51	0.39	0.38	0.54	0.50
2017	0.66	0.68	0.45	0.64	0.52	0.57
2018	0.58	0.66	0.41	0.58	0.52	0.61
Average	0.55	0.59	0.37	0.50	0.67	0.63
Std. Dev.	0.06	0.08	0.11	0.14	0.11	0.06

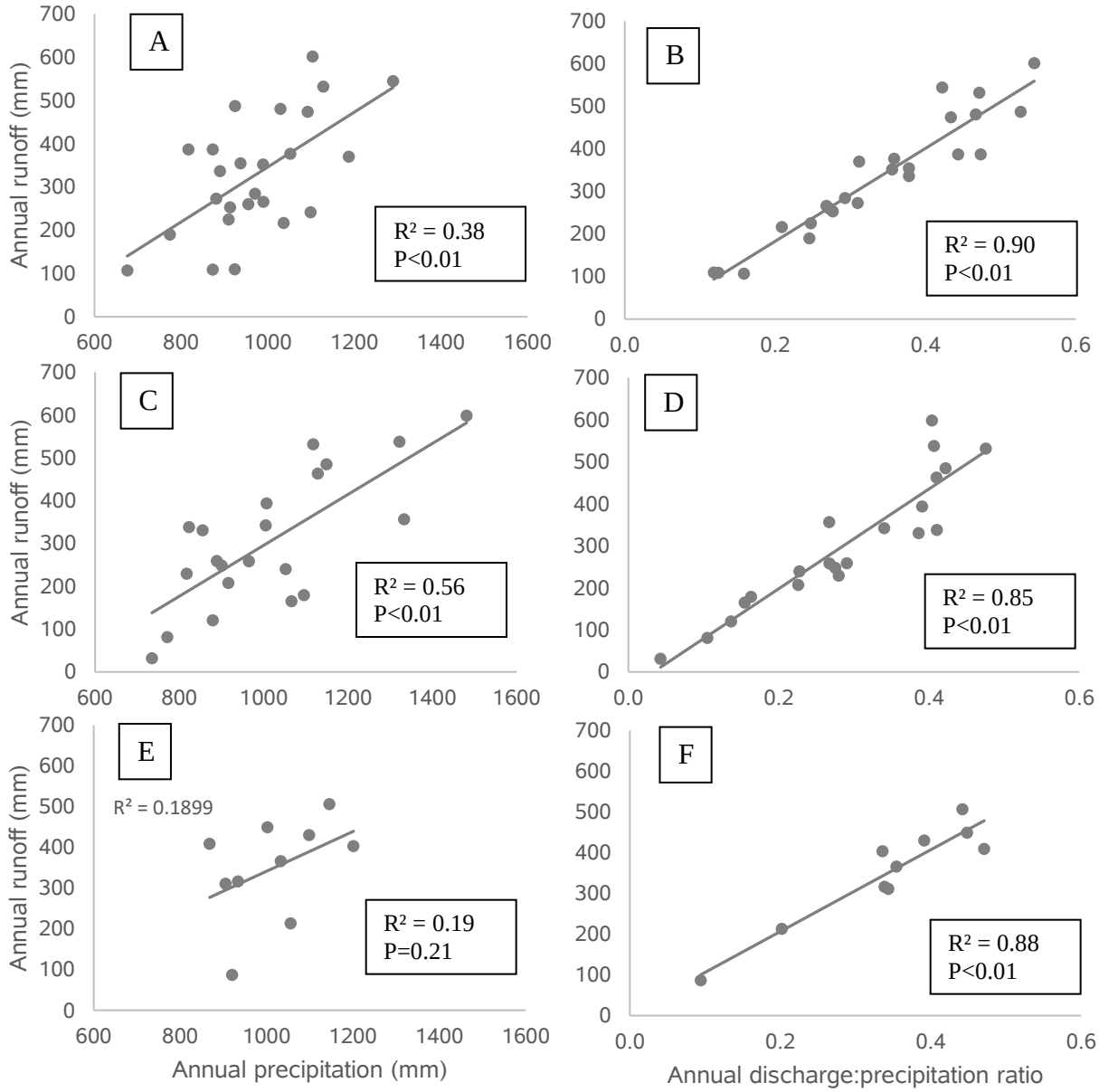

Figure B1. Relationship between annual runoff with annual precipitation and annual runoff:precipitation ratio at A & B) Embarras River (EMC), C & D) Lake Fork – Kaskaskia River (LFK), and E & F) Salt Fork River (SF) watershed.

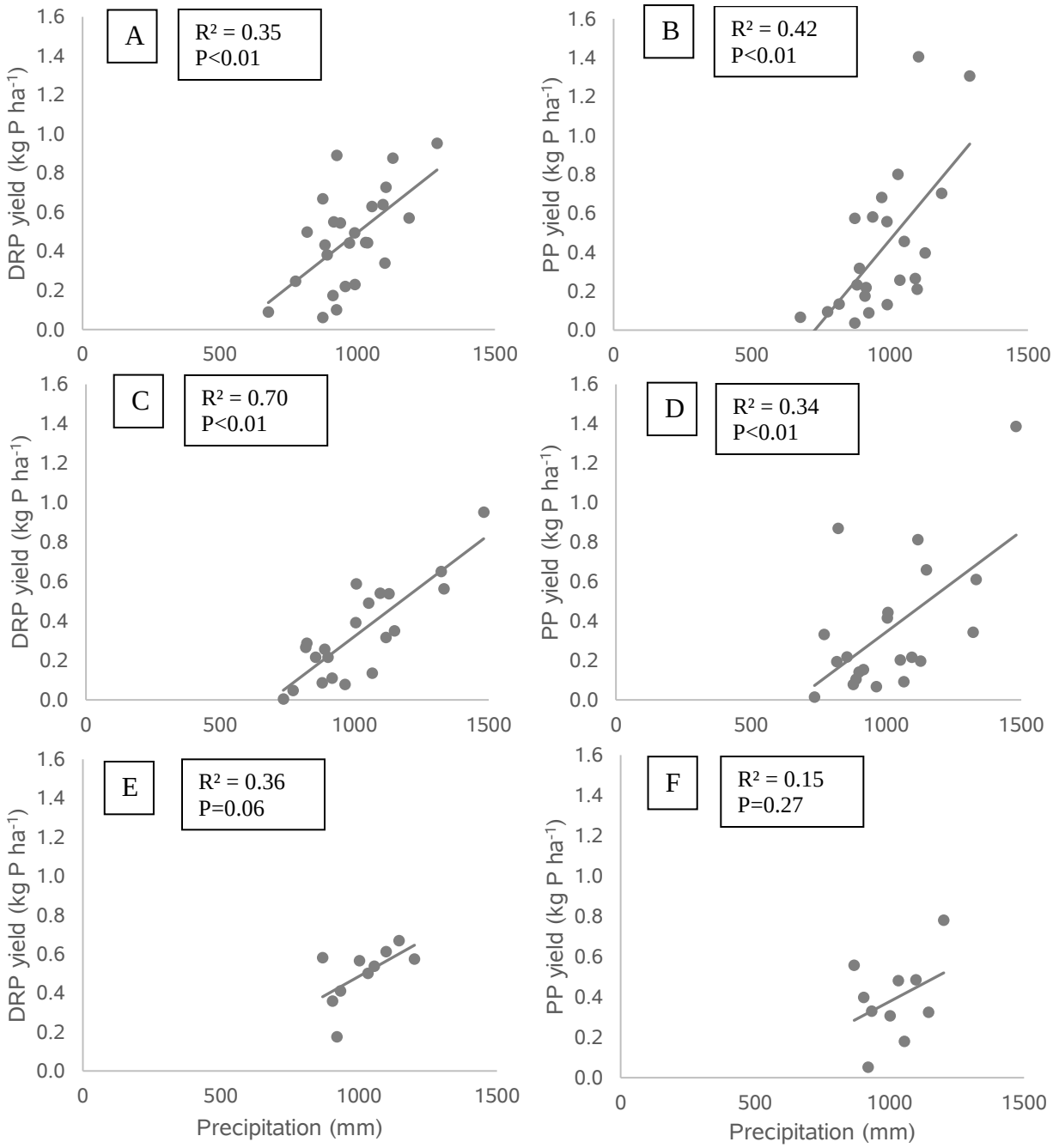

Figure B2. Relationship between annual dissolved reactive P (DRP) and particulate P (PP) yields with annual precipitation at A & B) Embarras River (EMC), C & D) Lake Fork – Kaskaskia River (LFK), and E & F) Salt Fork River (SF) watershed.

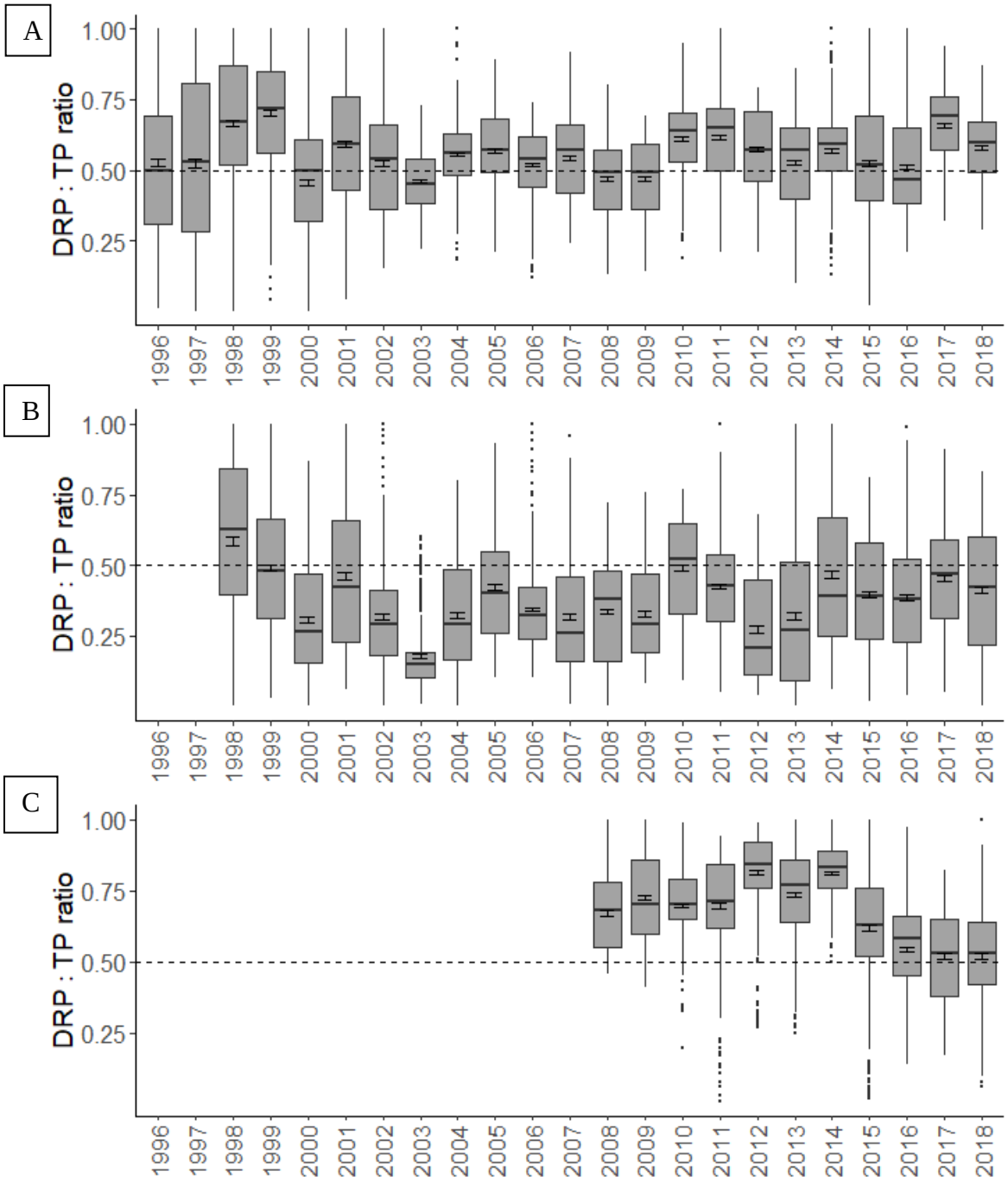

Figure B3. Daily DRP:TP ratios at A) Embarras River (EMC), B) Lake Fork - Kaskaskia River (LFK), and C) Salt Fork River (SF). Includes the entire dataset.

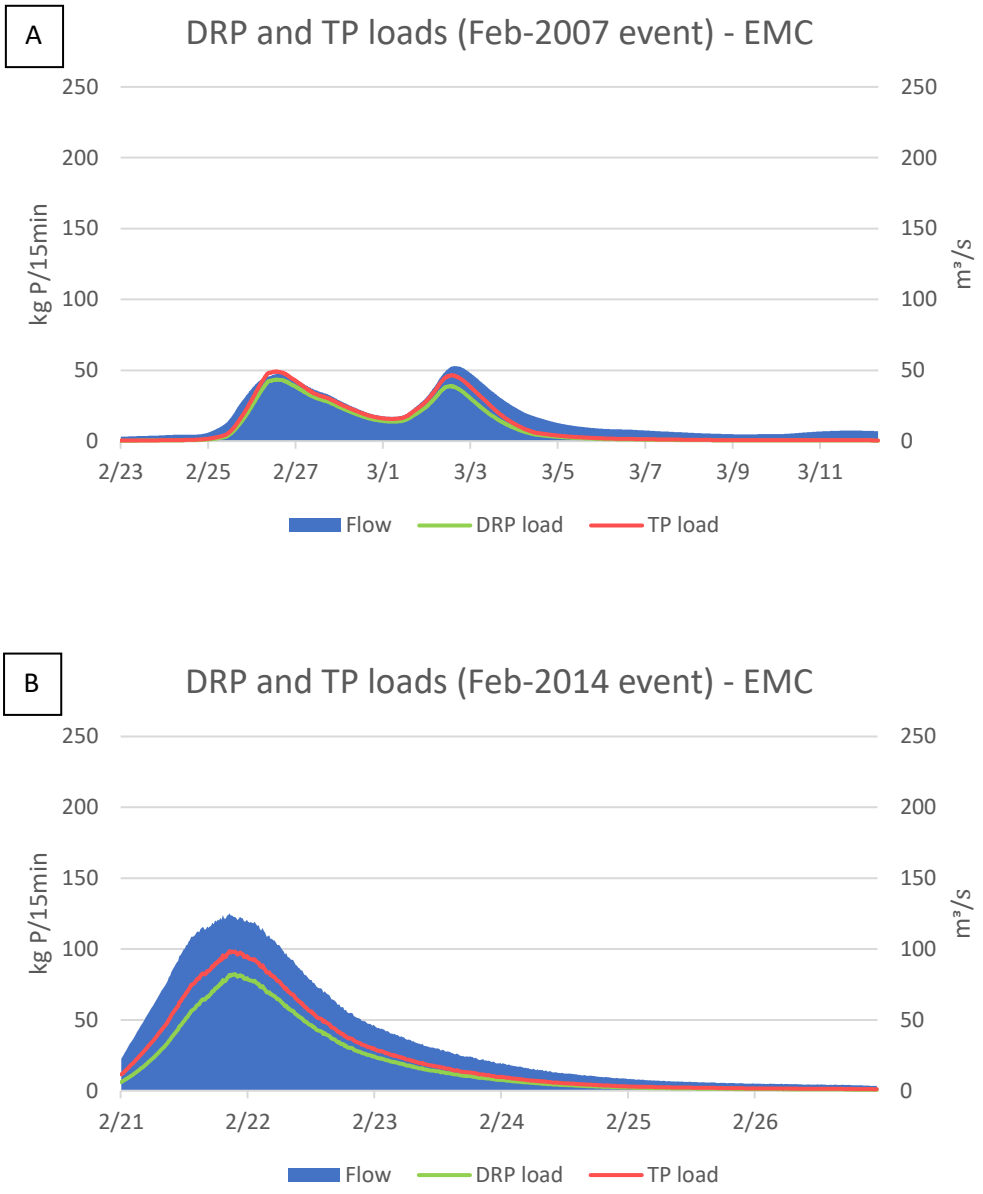

Figure B4. Dissolved reactive P and total P losses from two snowmelt events in A) February 2007 and B) February 2014 at Embarras River.